



# TECHNOLOGICAL DEVELOPMENTS SINCE THE DEEPWATER HORIZON OIL SPILL

By Nilde Maggie Dannreuther, David Halpern, Jürgen Rullkötter, and Dana Yoerger

Guillaume Novelli deploys the eco-friendly CARTE drifters, which are designed to measure shallow-depth surface currents. *Photo credit: Cédric Guigand*

“Although mitigation measures were planned for and ready at hand, the severity and unusual circumstances of the [Deepwater Horizon] accident called for the development of new techniques and approaches, as well as the improvement of existing methods, for mitigation and for investigations of the fate and impacts of the released material and the physical, chemical, and biological processes involved.”

**ABSTRACT.** The Gulf of Mexico Research Initiative (GoMRI) funded research for 10 years following the Deepwater Horizon incident to address five themes, one of which was technology developments for improved response, mitigation, detection, characterization, and remediation associated with oil spills and gas releases. This paper features a sampling of such developments or advancements, most of which cite studies funded by GoMRI but also include several developments that occurred outside this program. We provide descriptions of technological developments, including new techniques or the novel application or enhancement of existing techniques, related to studies of the subsurface oil plume, the collection of data on ocean currents, and oil spill modeling. Also featured are developments related to interactions of oil with particulate matter and microbial organisms, analysis of biogeochemical processes affecting oil fate, human health risks from inhalation of oil spill chemicals, impacts on marine life, and alternative dispersant technologies to Corexit. Many of the technological developments featured here have contributed to complementary or subsequent research and have applications beyond oil spill research that can contribute to a wide range of scientific endeavors.

## INTRODUCTION

Over a 10-year period following the Deepwater Horizon (DWH) incident, the independent Gulf of Mexico Research Initiative (GoMRI) funded a variety of efforts to better understand its impacts and to be better prepared for future oil spills. GoMRI-funded studies addressed five research themes, one of which was technology developments for improved response, mitigation, detection, characterization, and remediation associated with oil spills and gas releases. The purpose of this paper is to provide a sampling of technological developments, including new techniques or the novel application or enhancement of existing techniques. Most of the featured developments cite studies funded by GoMRI, but several of them occurred outside this program (see

the acknowledgments in the cited literature for funding details).

The selection of technological developments for this paper began with a decision to focus on those described in GoMRI-funded publications. We reviewed publications whose authors associated their studies with the program's research theme of technology, and also conducted a limited review of publications associated with the four other program themes whose titles, abstracts, or methods suggested possible technological advancements. This survey yielded about 250 potential candidates, which were further reduced by the elimination of studies that broadly discussed or assessed technology, were theoretical in nature, lacked clarity of an innovation, or lacked a clear applica-

tion for oil spill research. We then applied our expertise in organic chemistry, ocean physics and engineering, and oceanic-atmospheric processes to identify developments that moved oil spill science forward. We further eliminated advancements related to the tracking and analysis of oil spill components and transformation products (discussed in Rullkötter and Farrington, 2021, in this issue) and those concerned with improvements to ocean circulation modeling (discussed in Boufadel et al., 2021, in this issue). This process ultimately resulted in the 37 technological developments featured here that broadly reflect the scope of the GoMRI program. We acknowledge that the selection process and space constraints necessitated the exclusion of important and interesting innovations that have occurred since the DWH oil spill.

Brief paragraph-style summaries for each development are provided below, organized by broad topics. Each summary states what the development or innovation is or does, followed by a few details germane to its function and, in some cases, the main knowledge or insight that is intended by or that resulted from its use. In a few instances, examples are given of complementary or subsequent research that followed the innovation. We hope that by highlighting these few developments, readers will be enticed to learn more about them and seek out other technological advancements.

## DEVELOPMENTS IN INVESTIGATING OIL PLUME DYNAMICS

In contrast to shallow-water or surface oil spills, a deepwater hydrocarbon blowout releases oil and gas as a buoyant jet in high-pressure, cold-temperature conditions. As the jet interacts with the surrounding marine environment, it evolves into plumes of differently sized and distributed droplets, as happened during the DWH incident. Some of these droplets move upward and form surface slicks, and others are trapped in a neutrally buoyant plume that moves beneath the ocean's surface. Any of these droplets may later form surface slicks or attach to floating marine snow and sink to the seafloor near to or at a distance from the source site.

Understanding and quantifying the factors that affect a submerged jet's evolution is critical to estimating the amount of oil released and predicting where it will go. Simulation studies investigating droplet breakup and coalescence in turbulent flows are not new, but research on the DWH incident included factors not typically accounted for, such as Macondo oil chemistry and flow rates, dispersants applied at depth, high pressure, cold temperature, and biodegradation.

Innovations featured here characterize the subsurface oil plume and droplet size distributions (DSDs) resulting from a deepwater hydrocarbon release. Also featured here are instruments that measure oil droplets and gas bubbles in laboratory and field settings, which, in the case described below, are two natural seafloor seeps at depths similar to the DWH blowout site. Natural hydrocarbon seeps provide a viable surrogate for studying the subsea plume that formed during the DWH incident because both have bubbles and droplets that are well separated in water and end up with low dissolved gas concentrations at nearly ambient temperature and pressure. Topics related to oil plume dynamics are also discussed by Rullkötter and Farrington (2021), Boufadel et al. (2021), and Farrington et al. (2021), all in this issue.

Existing technologies were applied in an innovative way to characterize the DWH subsurface oil plume, a phenomenon first discovered by Diercks et al. (2010) and linked to the DWH incident. To collect environmental data in the area of the reported subsurface plume, Camilli et al. (2010) used a Doppler water velocity log and a mass spectrometer on board the autonomous underwater vehicle (AUV) *Sentry* to record current speeds and chemical parameters and also used a ship-cabled rosette sampler to collect water samples. Results from these data indicated the presence of a continuous, neutrally buoyant plume that had not substantially biodegraded at heights up to 200 m, depths down to 1,160 m, and, in certain areas, across horizontal distances of more than 2 km. The plume was found to be moving along a southwesterly trend more than 35 km from its source, likely influenced by Lagrangian transport and topography. Later, Valentine et al. (2014) analyzed 17 $\alpha$ -hopane concentrations (a degradation-resistant proxy for Macondo's liquid-phase oil) available in a public sediment database to assess the spatial distribution of hydrocarbons. Their analyses revealed an oblong patchwork of contamination spanning 3,200 km<sup>2</sup> that trended primarily to the west from the DWH site to a distance of at least 40 km, in agreement with observations reported by Camilli et al. (2010). Together, these innovative efforts characterized the plume's chemical parameters as well as significant transport and fate processes that were not originally accounted for in the DWH oil budget.

A few examples of research that followed the collection and analysis of samples from the oil plume include the work of Kujawinski et al. (2011), who corroborated findings on the fate of the Corexit component DOSS (dioctyl sodium sulfosuccinate), and Reddy et al. (2012), who extended the chemical analyses to a wider range of oil spill chemicals. Socolofsky et al. (2011) used the observations in calculations for a multiphase plume model that simulated the forma-

tion of subsurface oil intrusions. These calculations were subsequently used by Zhao et al. (2014b) as parameterizations in the jet-droplet formation model VDROP-J (see below) to simulate DSDs as oil evolves away from a jet, by North et al. (2015) in a coupled model to assess the influence of biodegradation and initial droplet sizes on subsurface oil transport, and by Aman et al. (2015) in a high-pressure sapphire autoclave apparatus to study oil-in-water dispersions.

Zhao et al. (2014b) extended the droplet formation model VDROP (Zhao et al., 2014a), developing the VDROP-J model that includes a new jet module calibrated with different orifice sizes and velocities to estimate the size distribution of droplets as they evolve from a buoyant jet stream. The VDROP-J model was validated under various conditions, such as with oil-only experiments conducted at SINTEF and with field data from the Norway offshore experiment and the DWH incident. Simulations with dispersants (10- and 1,000-fold reduction in interfacial tension) incorporated Macondo oil and gas release information and seawater conditions during the DWH spill. Both dispersant cases resulted in an increased volume of small droplets and decreased size distributions at different plume heights that correlated well with field data. These simulations indicate that droplet breakup processes mainly occurred within 50 m above the seafloor and reached a steady state at ~100 m and maintained that state to 200 m (representing the near-field upper boundary). The new jet module accounts for resistance to breakup by the oil's viscosity, which is important when dispersants are used, improving near-field simulations of DSDs from a deepwater blowout.

Research that utilized the VDROP-J model includes Zhao et al. (2015) to provide bounds on the range of droplet sizes from within 200 m of the DWH site; Zhao et al. (2017) to develop a new formulation for the simultaneous simulation of bubble and droplet size distribution; and Boufadel et al. (2018) to study the

dynamics of oil and gas tumbling within the pipe from which the oil emanated, the results of which have implications for estimations of discharged oil amounts.

Dissanayake et al. (2018a) developed the Texas A&M Oil Spill/Outflow Calculator (TAMOC), a comprehensive fluid dynamics and oil chemistry model that runs scenarios with and without dispersants to assess oil and gas ejected in deepwater (~1,500 m) spills, such as occurred at the DWH platform. The suite has a discrete particle model (DPM), a Lagrangian particle model, and two plume modules: the stratified plume model (still or near-still environments) and the bent-plume model (crossflow). The DPM computes the physical, thermodynamic, and oil chemical properties to predict the evolution from live oil (with dissolved gas) to dead oil (volatile components removed). Simulations were in line with field observations (DeepSpill experiment), Macondo oil properties, and laboratory data (bubble plumes and bubbly and oily jets). TAMOC simulations confirmed that the approach used in oil spill models is often correct, but its rigorous chemistry model and well-described methods are advancements that recent response-type fluid dynamics models do not include.

The General NOAA Operational Modeling Environment in Python (PyGNOME) adopted the TAMOC for near-field subsurface oil spill modeling. Other examples of research that utilized TAMOC include Gros et al. (2017) who, in combination with the VDROPI model, simulated the physical and chemical behavior of oil and gas rising to the surface with and without dispersants. TAMOC was utilized by Dissanayake et al. (2018b) to simulate marine oil snow formation and evolution, by Socolofsky et al. (2019) to simulate biodegradation in subsurface oil spills, by Gros et al. (2020) to explain the observed dynamics of live and dead oil droplets under deepwater conditions, and by Razaz et al. (2020) to connect the characteristics of a hydrocarbon seep to its surface footprint.

Lindo-Atichati et al. (2016) added

a new oil module to the coupled Connectivity Modeling System (CMS, biodegradation included) and to the Gulf of Mexico Hybrid Coordinate Ocean Model (HYCOM) to evaluate the influence of hydrodynamic, thermodynamic, and geochemical factors on the evolution of the subsurface oil plume. The oil module incorporated hydrocarbon fractions for Macondo oil and daily oil flow rates from field measurements. Adding variable flow rates provided more realistic initial conditions and enhanced the coherence of the southwest branch of the subsurface plume. Adding biodegradation rates at high pressure resulted in estimates of droplet size and density that led to increased residence time of the oil in the water column. The model predicted a persistent subsurface plume southwest and northeast of the DWH site at 1,100–1,200 m depths consisting of droplet sizes of >50  $\mu\text{m}$  (droplets in the 50–100  $\mu\text{m}$  range formed shallower plumes) during the first 100 days after the spill, in agreement with observational studies.

The CMS with oil application was used,

for example, by Berenshtein et al. (2020) to identify the spill exposure area that was beyond the satellite-identified boundaries of the DWH footprint and fishery closures and by Perlin et al. (2020) in case studies that investigated parameters that affect oil weathering and transport, confirming the system's robustness for simulating a deep-sea blowout.

Aman et al. (2015) employed a high-pressure sapphire visual autoclave apparatus to estimate oil droplet diameter as a function of mixing speeds (Figure 1). The apparatus provided the first visualizations of droplet breakup and coalescence at turbulent kinetic energy dissipation rates corresponding to 200–1,000 rpm mixing speed (Booth et al., 2019) and up to 120 times atmospheric pressure (roughly the pressure at 1,200 m depth). A high-speed camera enabled quantitative assessments of droplets. The data were used in DWH simulations (using the coupled CMS and Gulf of Mexico HYCOM) that showed a mean diameter size of 258  $\mu\text{m}$  at speeds up to 400 rpm. When speed increased ( $\geq 500$  rpm), droplet size decreased to an average of 80  $\mu\text{m}$ ,

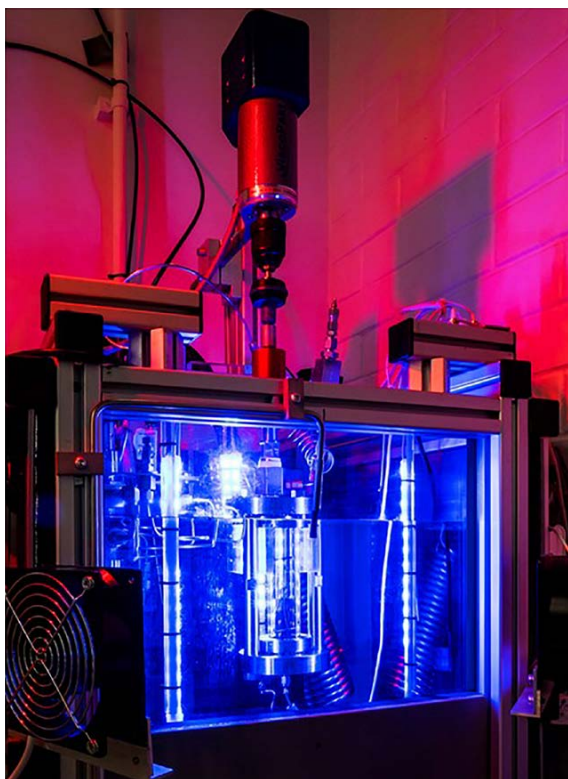


**FIGURE 1.** A high-pressure sapphire visual autoclave apparatus was utilized to help characterize the droplet size distributions that occurred during the Deepwater Horizon (DWH) incident (Aman et al., 2015). The autoclave provided the first visualizations of droplet breakup and coalescence at dissipation rates corresponding to 200–1,000 rpm mixing speed (Booth et al., 2019) and up to 120 times atmospheric pressure (roughly the pressure at 1,200 m depth). The autoclave's well-defined shear geometry provides a unique perspective on droplet size prediction, and the data it generated helped establish a systematic approach for estimating the diameter of oil droplets dispersed in water. Photo used with permission of Zachary M. Aman, The University of Western Australia

suggesting a natural mechanism for oil to disperse into small droplets. The autoclave's well-defined shear geometry provides a unique perspective on droplet size prediction, and the data it generated helped establish a systematic approach for estimating the diameter of oil droplets dispersed in water.

Examples of research that utilized DSD estimations from the autoclave apparatus include Ainsworth et al. (2018) in the Atlantis ecosystem model to simulate oil spill impacts on fish guilds and their subsequent recovery and Perlin et al. (2020) in case studies investigating parameters that affect the weathering and transport of deep-sea oil spills.

Wang and Socolofsky (2015) designed, validated, and deployed a deep-sea stereoscopic imaging system, TAMU-CAM, that was mounted on the remotely operated vehicle (ROV) *Hercules* to measure and analyze gas bubbles and oil droplets flowing from natural seeps (Figure 2). The system consists of two high-speed cameras in pressure housings (rated to 1,500 m depth), lighting, subsurface power, and video monitoring over ethernet. Images are streamed onto a 12 GB

RAM memory chip and transferred to a 240 GB flash drive in each camera from which the gathered information can be downloaded to a computer in the ROV, enabling almost unlimited data collection. Laboratory validation showed that the stereo view improved measurements of bubble diameters up to 90% and flow rate estimates by a factor of ~13% compared to single-camera systems. In the Gulf of Mexico, the system tracked oil droplets and gas bubbles up to ~250 m above two natural seep sites (and later up to 400 m; Wang et al., 2020). Imagery captured bubble and droplet breakup and coalescence from which size distribution, rise velocity, and methane flux were estimated, improving model parameterization for simulating deepwater spill scenarios.

Leonte et al. (2018) provide an example of research that utilized the TAMU-CAM observations, from which they established that changes in methane stable carbon isotopic ratios can be used as a tracer for methane dissolution. Their analysis using this tracer indicated that more than 90% of the methane released during the DWH spill dissolved after ascending 400 m.

## INSTRUMENTATION FOR IMPROVED OIL TRANSPORT PREDICTIONS

During the DWH incident, information that was critical for response decisions was provided by remote sensing (slick locations) and by ocean circulation models (slick transport). However, a need became evident for more accurate information about how the transport of floating oil is influenced by fast-moving submesoscale near-surface currents of short duration and their interactions with the mesoscale Loop Current that moves water through and out of the Gulf of Mexico, around the tip of Florida, and into the Atlantic Ocean. This need points to an ongoing challenge in ocean circulation modeling—the limited availability of observational data to initialize predictive models. The following text describes instrumentation advancements aimed at collecting data about the ocean's near-surface currents that can be used to improve the parameterization of transport prediction models. For a discussion on the modeling of geophysical ocean transport processes, see Boufadel et al. (2021, in this issue).

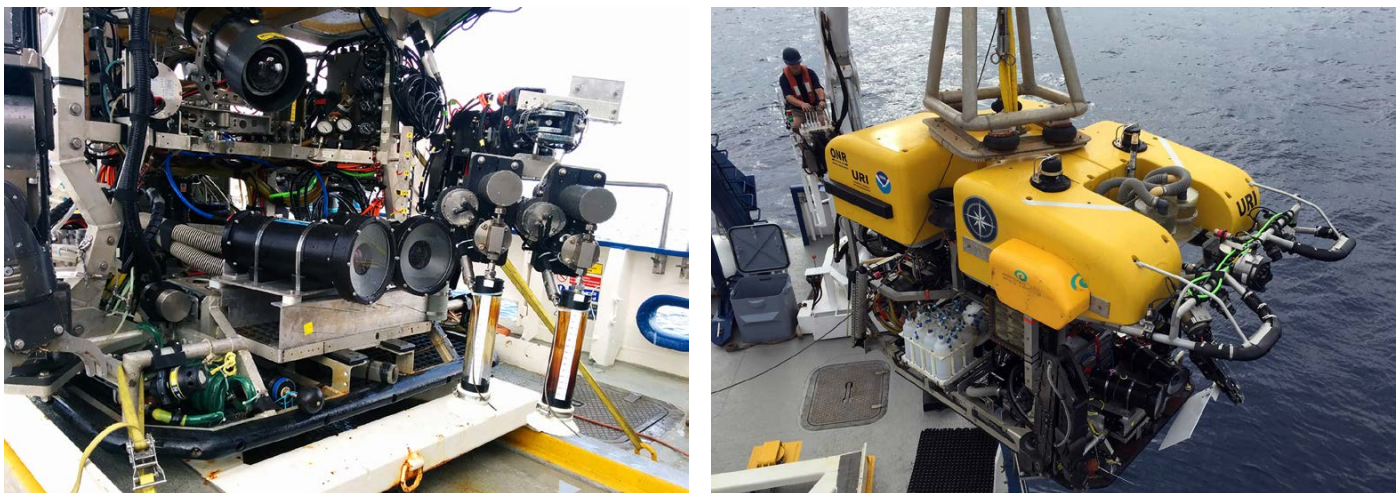


**FIGURE 2.** To help characterize the subsurface oil plume and droplet size distributions that resulted from the DWH incident, researchers investigated oil droplets and gas bubbles flowing from deep natural seafloor seeps, which provide a viable surrogate for studying the subsea plume that formed during the DWH incident. They used the remotely operated vehicle (ROV) *Hercules*, shown at right, to deploy the Texas A&M University stereoscopic high-resolution camera system (TAMU-CAM), pictured at left, which was developed to collect fine-scale images and measurements of oil droplets and gas bubbles rising from the seeps (Wang and Socolofsky, 2015). TAMU-CAM features two high-speed cameras within housings rated to 1,500 m depth and has its own lighting, subsurface power, and video monitoring over ethernet that can be downloaded to a computer in the ROV. *Photo on the right by and used with permission of Binbin Wang, Civil and Environmental Engineering, University of Missouri. Photo on the left by and used with permission from Scott Socolofsky, Texas A&M University*

Novelli et al. (2017) developed the Consortium for Advanced Research on Transport of Hydrocarbon in the Environment (CARTHE) drifter to facilitate large-scale observations of near-surface ocean currents and improve ocean model parameterization. The easy-to-assemble CARTHE drifter can be mass produced at low cost and is made from a biodegradable polymer produced by sugar-fed bacteria to reduce ocean pollution. A floating torus (Figure 3) houses a global positioning system and alkaline batteries, and a four-sail drogue attached with a flexible connector keeps the floater upright on waves. Without the drogue, the floater moves at wave speed; with the drogue, it moves at the underlying current speed. Tests with small-scale models were conducted in a wind-wave-current flume, and tests with full-scale models during the LAGrangian Submeso-scale ExpeRiment (LASER) field campaign (<http://carthe.org/laser/>) validated trajectories against a well-established drifter model.

After the LASER field experiment, D'Asaro et al. (2018) reported that small fronts and vortices caused the drifters to cluster at frontal convergence zones and that larger currents distributed the drifters over a wide region later. Their results suggest that floating oil might accumulate similarly, potentially providing a window of opportunity for a targeted deployment of resources during a spill response. Results from a different field experiment using CARTHE drifters and other observational devices were reported by Androulidakis et al. (2018), who identified the influence of local and regional physical processes such as riverine fronts on the transport of surface oil from the Taylor Energy site.

Examples of research that used data collected by CARTHE drifters include Lund et al. (2018) to validate near-surface current maps generated from shipboard marine X-band radar, Barkan et al. (2019) to validate model estimations of vertical buoyancy fluxes during frontogenesis, and Gonçalves et al. (2019) to

identify and follow a near-surface flow that was reconstructed by a supervised machine-learning technique using only Lagrangian data. Additionally, Novelli et al. (2020) investigated the trajectories of the DWH oil spill and the CARTHE drifters released during the LASER experiment and found that near-surface gradients controlling cross-shelf movement transported the undrogued drifters twice as fast as the drogued ones, and a higher percentage of undrogued drifters landed on the same coastline locations where DWH oil was found.

Laxague et al. (2018) employed a novel combination of instruments with complementary strengths that mitigated each instrument's blind spot to obtain the first-of-their-kind field observations in the ocean's upper layers (~10 m depth). Wind forcing and wave dynamics strongly influence motion in the upper layers, but analyses of near-surface dynamics generally treat these upper layers as the same because it is challenging to observe and measure currents within this area. As such, it is difficult to accurately predict the transport of buoyant materials such as microplastics and oil. This observation gap was addressed in a case study during the



Submesoscale Processes and Lagrangian Analysis on the Shelf (SPLASH) field campaign (<http://carthe.org/splash/>) that collected data simultaneously with several sensors and instruments, including a polarimetric camera (for wave motion and depth), a 20 MP camera attached to a drone (that tracked drifters and bamboo plates), an autonomous vehicle-mounted acoustic Doppler current profiler (ADCP) and shipboard ADCP (for currents deeper than 4 m), a mast-mounted sonic anemometer (for wind velocity), and bow-mounted acoustic altimeters (for water-surface elevation). The data revealed that wind forcing caused the current at 1 cm depth to move at twice the average speed over the upper 1 m and nearly four times the average speed over the upper 10 m. These results help account for the rapid separation of floating material of varying size or buoyancy. Incorporating these quantified dynamics into ocean transport forecasts can aid in identifying pathways along which floating material may be transported.

To improve the accuracy of ocean model parameters, Carlson et al. (2018) collected the first modern in situ observations of small-scale surface dispersion

**FIGURE 3.** During the DWH incident, a need was revealed for more accurate information about the influence that complex upper-ocean currents have on oil transport. To better understand these fast-moving, short-lasting currents, field experiments were conducted in the Gulf of Mexico and used the new Consortium for Advanced Research on Transport of Hydrocarbon in the Environment (CARTHE) drifter, which is easy to assemble, has a low production cost, and is biodegradable (Novelli et al., 2017). The drifter is made from a polymer produced by sugar-fed bacteria. A global positioning system and alkaline batteries are housed in its floating torus, and a four-sail drogue attached to the torus with a flexible connector keeps the floater upright on waves (see photo on opening page of this article). During field experiments, the CARTHE drifters clustered along fronts, and then later dispersed, suggesting that floating oil might accumulate similarly and identifying a possible window of opportunity for a targeted deployment of resources during a spill response (D'Asaro et al., 2018). *Image by and used with permission of Cédric Guigand, University of Miami*

in a deepwater setting with the custom-outfitted Ship-Tethered Aerostat Remote Sensing System (STARSS; **Figure 4**). Velocities at the air/sea interface and dispersion for short-lived motions (seconds to hours) at small spatial scales (meters to hundreds of meters) are relevant to oil drift and spread, but these parameters are challenging for drifters, ships, and satellites to observe. Data were collected during the CARTHE LASER field campaign using the STARSS equipped with a 50.6 MP camera (300 × 200 m field of view) that imaged floating bamboo plates every 15 s for 4 h. A relative rectification technique enhanced image analysis by minimizing movement between frames, then custom algorithms quantified dispersion; drifter trajectories were used to

connect small-scale features to the sub-mesoscale. Results improved diffusivity estimates at the 3–40 m scale and revealed that density fronts and Langmuir circulation directed a preferred motion at small spatial and short temporal scales (Chang et al., 2019), which are difficult to reproduce in numerical ocean models.

## OIL SPILL MODELING TECHNIQUES

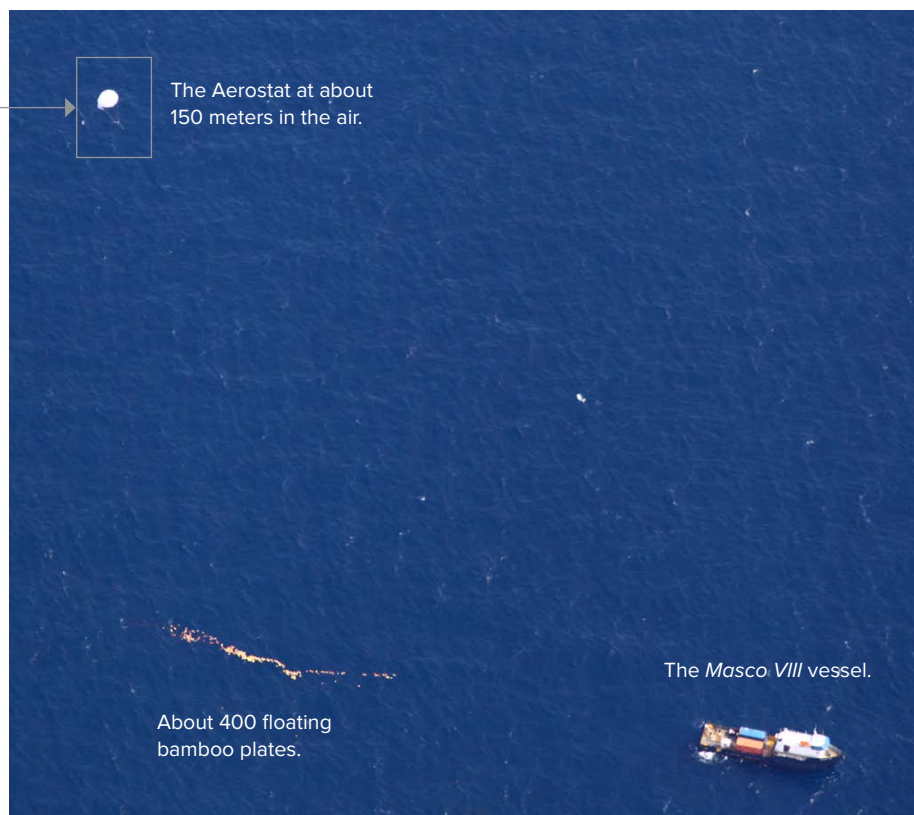
Advancements in oil spill modeling following the DWH incident are discussed by Barker et al. (2020) in their review of operational modeling in support of oil spill response. Here, we describe two additional modeling suites, one that tracks oil from its deepwater release to landfall and another that tracks the interactions of oil with marine organisms, biochemical constituents, and sediments. We also provide additional information about an oil drift module that is included in the Barker et al. (2020) review.

Chapman et al. (2014) constructed a nested model suite to follow an oil particle from its seafloor release to shore-

line arrival that includes natural rates of mixing, degradation of oil components, and processes at Gulf-wide, shelf, and bay scales. This technique addresses the need revealed during the DWH incident to have interacting systems at appropriate spatial scales and resolutions. The suite accounts for plume dynamics, including a density-stratified turbulent crossflow (with a three-dimensional Large Eddy Simulation-Reynolds Averaged Navier-Stokes model), an intrusion formation by density stratification (with an integral multiphase plume model with oil chemistry), and the behavior of discrete particles and dissolved constituents as oil ascends to the surface (with a Lagrangian particle tracking model with algorithms from the General NOAA Operational Modeling Environment). Two sets of models simulate surface transport from offshore to coastlines. The first set incorporates a base hydrodynamic model (that includes a high-resolution ocean-atmosphere model and the Weather Research and Forecasting model), the Regional Ocean Modeling System (ROMS), and the South



**FIGURE 4.** The complex processes in the upper ocean—which drifters, ships, and satellites have limited ability to observe—are relevant to oil drift and spread. To better understand near-surface ocean currents, the Ship-Tethered Aerostat Remote Sensing System (STARSS) was custom outfitted with a 50.6 MP camera (300 × 200 m field of view) and launched from a research vessel in the Gulf of Mexico to take images of floating bamboo plates every 15 s for 4 h. The data collected provided the first modern in situ observations of small-scale surface dispersion, and results improved diffusivity estimates at the 3–40 m scale, which can enhance the parameterization of ocean transport models (Carlson et al., 2018). Both photos by and used with permission of Tamay Özgökmen, University of Miami



Atlantic Bight and Gulf of Mexico model that assimilates sea surface height and temperature data from satellites. The second set comprises smaller-scale models, including the ROMS model of the Texas-Louisiana shelf that captures the interaction of mesoscale eddies with the continental slope as well as the currents on the shallower shelf and a three-dimensional nonhydrostatic coastal bay model. The nested model suite is supported by laboratory experiments (bubble and droplet formation, droplet-turbulence interaction, dissolution, evaporation, and dispersion) and field experiments (deep-sea tracer and bubble releases). Qualitative comparison with observations of the southwest-tending DWH subsurface plume showed good agreement. Simulations suggest Macondo oil released during the DWH incident may have also been transported in the subsurface to the east, but this could not be validated because sampling efforts were concentrated to the west.

Dukhovskoy et al. (2021) developed the Consortium for Simulation of Oil-Microbial Interactions in the Ocean (CSOMIO) coupled modeling system to simulate the distribution and interaction of petroleum, lower trophic level organisms, biochemical constituents, and sediment in the marine environment for assessing environmental effects of past and future oil spills. The system is based on the Coupled Ocean-Atmosphere-Wave-Sediment Transport (COAWST) modeling system (Warner et al., 2010) and consists of several components. The oil plume modeling component is coupled to the ROMS hydrodynamic model, which simulates the three-dimensional movement and compositional changes (weathering) of oil as Lagrangian particles. The chemical composition of oil is described in terms of saturates, aromatics, and heavy oil (including resins and asphaltenes). The biogeochemical modeling component incorporates a microbial model based on the Genome-based Emergent Ocean Microbial Ecosystem (Coles et al., 2017) that was adapted for

the presence of hydrocarbons. The sediment transport component of COAWST, the Community Sediment Transport Modeling System, was modified to include computationally efficient flocculation parameterizations for oil-mineral aggregates developed from laboratory experiments. These modeling components are linked together using a two-way Lagrangian-Eulerian mapping technique that enables interaction among the model components to track hydrocarbons from a source blowout to deposition in sediment and to account for microbial degradation and evaporation during transport through the ocean. The CSOMIO model can be run offline at increased computational speed to support spill response.

Dagestad et al. (2018) developed OpenDrift, a high-resolution open-source circulation ocean trajectory framework that contains the OpenOil oil drift module, which was improved, extended, and applied to modeling the DWH oil spill. Simple to set up, the independent and fast OpenDrift platform provides flexibility for scientific studies as well as robustness for operational services. The OpenDrift core includes everything common to ocean drift applications (e.g., search-and-rescue, plastics, and ichthyoplankton transport). The OpenOil module adds functionality specific for oil by including an interface with the NOAA OilLibrary (<https://github.com/NOAA-ORR-ERD/OilLibrary>) with measurements for ~1,000 oil types) and offers parameterization of weathering processes such as evaporation, emulsification, biodegradation, and entrainment by breaking waves followed by vertical turbulent mixing with buoyancy and resurfacing.

Examples of research that utilized the OpenDrift trajectory modeling framework include DWH spill simulations by Hole et al. (2019), which showed that a large river outflow reduced the total amount of stranded oil by ~50% compared with no river input; these results compared well with satellite observations of the DWH surface oil patch. Using OpenDrift to simulate oil spills

in the Cuban Exclusive Economic Zone, Androulidakis et al. (2020) showed the most likely scenario for oil stranding along the southern Florida coast would be from a release in the deep central Straits of Florida and, for oil stranding at Gulf of Mexico beaches, would be from a release near the Yucatán Strait and in the deep Gulf interior.

After adding functionality to the OpenOil module, Garcia-Pineda et al. (2020) employed it to initialize simulations of oil slicks near the Taylor Energy site for experiments aimed at understanding the residence time of oil slicks using a combination of remote-sensing platforms and GPS-tracked drifters. Although the projected oil residence times in low wind conditions were longer than observations, likely because the actual slick was very thin, this result demonstrates the importance of incorporating oil thicknesses into models.

## **ADVANCEMENTS IN STUDYING OIL, PARTICLE, AND MICROBIAL INTERACTIONS**

In both off- and near-shore environments, oil droplets in the water column can encounter floating matter, microbial organisms, and sediment particles, all of which can influence the oil's fate. In response to oil in their environment, some marine organisms excrete a sticky substance that may cause floating matter, sediment, and oil droplets to aggregate and sink to the seafloor. During the DWH incident, these processes were discovered to have a significant influence on the deposition of oil and dispersant to the seafloor. Advancements in collecting and analyzing images of suspended matter and in simulating the formation and evolution of oil/particle aggregates (OPAs), marine oil snow (MOS), and oil/mineral aggregates (OMAs) are featured below. Farrington et al. (2021, in this issue) also discuss topics related to interactions among oil and floating particulate matter and marine organisms.

The ability to distinguish between oil and gas droplets in a mixed release and to

quantify their distributions was achieved by Davies et al. (2017) with their new in situ particle imaging system, SilCam (Figure 5), designed to quantify high concentrations of suspended particles with diameters from 30  $\mu\text{m}$  to several millimeters. The SilCam's backlighting and telecentric receiving optics configuration provides sharp, in-focus images of all particles, free from errors associated with standard lenses. The optical configuration is mounted within two underwater housings (rated to 3,000 m depth), and images are recorded on a solid-state disk to enable continuous operation at 15 Hz without the need for buffering. The system's optical properties can distinguish between similarly shaped particles for analysis of oil droplets and gas bubbles and for establishing an oil/gas ratio. The SilCam fills a gap in technology that now allows accounting for the concentration-size-shape space within in situ particle measurement that can also be applied to study other suspended particles in the ocean.

Brandvik et al. (2017, 2019) utilized the SilCam in experiments using facilities at SINTEF, SouthWest Research Institute, and Ohmsett to distinguish oil and gas bubbles and calculate particle size distributions during simulated deepwater

releases of live oil and natural gas under high pressure, with and without subsurface dispersant injection.

Bi et al. (2015) customized a segmentation technique that locates objects within images and extracts them for classification to improve the processing of large volumes of data generated by plankton-imaging systems. Existing techniques worked for images acquired under laboratory conditions or within clear waters; however, the DWH incident underscored the need to process images from turbid coastal waters, where complex pathways transported oil toward shore. The two-step classifier procedure includes separating all non-target and target objects into different groups (arrow-like, copepod-like, and gelatinous zooplankton) and applying a support vector machine binary classifier (a supervised machine-learning method) to further identify non-target objects. Results using a test data set comprised of 89,419 images collected by the ZOOplankton VISualization (ZOOVIS) system in the Chesapeake Bay were consistent with visual counts, having >80% accuracy for all three object groups. This test demonstrated the technique's success in processing in situ imaging data collected in waters with large amounts of suspended matter.

This segmentation technique was utilized by Shahrestani et al. (2017) to analyze sonar footage of swimming fish and improve estimations of fish abundance at a fixed location. Cheng et al. (2019) drew upon the technique to develop and test an enhanced convolutional neural network for improved plankton image recognition that can be applied to images acquired from different systems.

Zhao et al. (2016) developed the A-DROP model to simulate the formation of OPAs and to predict how much oil from a marine spill an OPA might trap and transport. Application of a unique oil/particle coagulation efficiency formula to quantify the amount of oil that OPAs trap accounts for effects of particulate coating on an oil droplet's surface and effects of hydrophobicity and particle-to-droplet size ratio on OPA formation. After validating that the A-DROP model closely reproduced the oil-trapping efficiency reported in experimental studies, OPA formation was simulated in a coastal marine environment. Results suggested that although the increased particle concentration in the swash zone (the turbulent water layer that washes onto the beach) generated an increase in oil/particle interactions, it did not result in a corresponding increase in the amount

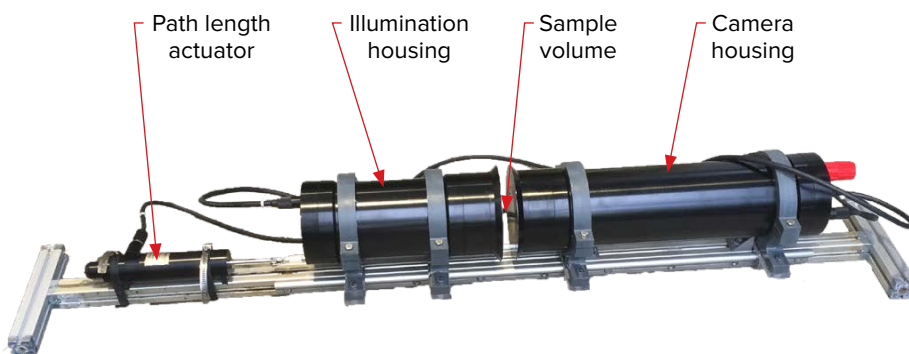


**FIGURE 5.** The SilCam in situ particle imaging system can distinguish between oil and gas droplets and quantify their distributions from a mixed release, as happened during the DWH incident (Davies et al., 2017). The SilCam (above) has an adjustable path length that ensures all suspended particles in the sample are in focus and utilizes signatures of transmitted light of different wavelengths through each particle to separate oil droplets, gas bubbles, and oil-coated gas bubbles of equal size and shape. The optical configuration is mounted inside of two underwater housings rated to 3,000 m depth. SINTEF senior engineer Frode Leirvik (left) prepares the SilCam for experiments at the Ohmsett National Oil Spill Response & Renewable Energy Test Facility in New Jersey. Both images provided by and used with permission of Emlyn Davies, SINTEF Ocean

of oil that OPAs trapped. The A-DROP's predictive capability for oil removal by OPAs, something that existing oil/particle models do not perform, advances this developing field of study.

The A-DROP model was utilized by Jones and Garcia (2018) in the development of a rapid response model for an oil spill in a riverine environment, and by Boglaienko and Tansel (2018) to characterize and classify different types of oil-particle aggregates as they developed oil spill response and mitigation methods.

Based on the success of earlier baffled recirculating tanks (BRTs; Knap et al., 1983), Wade et al. (2017) designed new versions of the tanks that reliably and efficiently produced large volumes of water-accommodated fractions (WAF) and chemically enhanced water-accommodated fractions (CEWAF) of oil for mesocosm studies to examine MOS formation. The BRTs produce  $\geq 500$  L of WAF and CEWAF within 24 h, which existing BRTs could not do, so that experiments can run in triplicate and provide sufficient exopolymeric substances for analyses. Each  $43 \times 88 \times 44$  cm glass tank contains four glass baffles (130 L total volume) and recycles water in  $\sim 6$  h using a diaphragm pump and a magnetic stirrer. A high-speed camera with a 200 mm lens measures the size distributions of resulting oil droplets. MATLAB Imaging Processing Toolbox software was applied to reduce the impact of non-uniform background intensity. Oil concentrations in the WAF and CEWAF treatments were consistent with environmental concentrations (higher range) seen during spills (including DWH), providing data for models that estimate oil sedimentation and degradation.

The BRTs were used by Doyle et al. (2018) in mesocosm experiments designed to study the relationship among microbial community structure, oil and Corexit, and MOS in coastal surface waters; by Bacosa et al. (2020) to investigate the concentration and distribution of hydrocarbons in marine snow aggregates; and by Shi et al. (2020) to determine the

half-lives of individual hydrocarbons in simulated oil spill scenarios with and without dispersant.

Ye et al. (2018) modified the high-resolution floc video instrument LabSFLOC by adding parameters to simulate the formation and settling of OMAs and study their effect on vertical oil transport. The modified LabSFLOC-2 system includes a 2 MP video camera and an LED-illuminated panel behind a settling column into which a suspension containing oil-mineral-microbial flocs is introduced. A digital video microscope and processing package enables detailed observations of individual floc size (5  $\mu\text{m}$  to 8 mm), shape, settling velocity, density, mass, and more. Preliminary laboratory experiments demonstrated that LabSFLOC-2 can produce OMAs and characterize their mass settling dynamics, allowing for a systematic analysis of the role that each factor plays in this process. Knowledge of quantitative floc properties of OMAs can improve the parameterization and calibration of numerical models that include oil biodegradation when forecasting the fate of oil spills.

Research that utilized the LabSFLOC-2 includes work by Dukhovskoy et al. (2021) to provide flocculation parameterizations for their coupled modeling system that simulates the distribution and interaction of petroleum, lower trophic level organisms, biochemical constituents, and sediment in the marine environment. Also, Ye et al. (2020) employed LabSFLOC-2 to investigate the effect of mineral types (kaolinite and bentonite) on the structure of OMAs and settling velocities.

Dissanayake et al. (2018b) developed a numerical modeling technique to predict the formation of MOS aggregates and the amount of oil they transport to the seafloor. The technique is based on the Stochastic Lagrangian Aggregate Model for Sinking Particles that simulates marine particle coagulation and disaggregation. Modifications were made to characterize aggregates containing different amounts of oil, algae, and sediment particles and to incorporate seawater

properties, stratification effects on aggregate settling velocities, disintegration, fractal dimensions, and stickiness. The model was validated with observational data collected during the DWH incident, and it was found to reproduce aggregate size spectra and oil deposition rates reasonably well. Oil spill transport and fate models do not typically account for oil sedimentation via MOS, as this phenomenon was not widely observed or studied prior to the DWH incident; therefore, this technique helps fill that gap by identifying and calculating aggregate parameters for MOS formation and sinking, which can inform calculations of oil fate in marine environments.

Passow et al. (2019) provide an example of research that further supports this MOS modeling technique. They conducted rolling table experiments that investigated the incorporation of two types of dispersed oil into diatom aggregates to provide specific input parameters for models that predict the transport of oil to depth via marine snow-sized aggregates. Another example can be found in Daly et al. (2020), who recommended coupling circulation and MOS models (that include coagulation as described above) to improve the predictions of MOS sedimentation events under varying environmental conditions.

## **DEVELOPMENTS IN COLLECTING AND ANALYZING BIOGEOCHEMICAL DATA**

There is limited understanding of the biogeochemical properties and physical processes that can influence the transport and fate of oil in deep-ocean environments such as the Gulf of Mexico location of the DWH incident. Here, we feature techniques that link the ocean's biochemical structure to physical conditions that are influenced by atmospheric conditions, which have a combined effect on oil fate. We also discuss a technique used to analyze sediments near the DWH site that led to estimations of the amount of oil that settled to the seafloor. For developments in analytic chemistry techniques

applied to study the chemical composition of spilled oil and its transformation products, see Rullkötter and Farrington (2021, in this issue).

Shay et al. (2019) deployed state-of-the-art Autonomous Profiling Explorer floats with biogeochemical and electromagnetic sensors (APEX-EM, developed by Teledyne Webb Research) near the DWH site to map physical processes and biogeochemical properties that could influence oil dispersion. This effort linked, for the first time, the ocean's biochemical structure to physical conditions including currents and shear as influenced by atmospheric conditions. The deployed floats operated in 2–2,000 m depth for four-to-seven-day intervals and utilized daily updated satellite remote-sensing products. The floats' payloads included sensors for temperature and salinity (Sea-Bird Electronics); dissolved oxygen (Aanderaa Optode 4330F); and chlorophyll, fluorescence, backscatter, and colored dissolved organic matter fluorescence with fluorophoric oil components (ECO Puck Flibb-CD). After the floats surfaced, data were transmitted via satellite (Iridium system), enabling real-time retrieval and reprogramming for adaptive sampling, which enabled an increase in the profiling rate during Hurricanes Irma and Nate. The floats also collected >1,600 continuous-mode samples of diurnal oxygen variations (Gordon et al., 2020). The easy-to-deploy end-to-end APEX-EM system measures evolving mesoscale structures, providing data needed for resolving submesoscale processes that are important to oil transport predictions.

Chanton et al. (2015) employed an inverse isotopic approach to measure radiocarbon ( $^{14}\text{C}$ ) in organic matter layered on the top of seafloor sediments and quantify sedimented oil following the DWH incident. The approach served as a proxy for oil spill-derived compounds, many of which had changed chemically from microbial and physicochemical processes and were no longer amenable to gas chromatographic analysis. This approach

is “inverse” in that it looks for the absence of  $^{14}\text{C}$ , which diminishes over time. Before the spill, there was a more recent  $^{14}\text{C}$  signature of organic matter derived from land-plant, riverine, and marine sources than there was after the spill deposited carbon from crude oil that was millions of years old with no  $^{14}\text{C}$ . Analysis of sediment collected shortly after the spill and around the site estimated that ~3%–4.9% of reported Macondo oil likely deposited on the seafloor, an estimate within the 1.8%–14.4% determined using a  $17\alpha$ -hopane biomarker tracer. Analysis of  $^{14}\text{C}$  instead of a stable carbon isotope composition ( $\delta^{13}\text{C}$ ) can distinguish crude oil from non-fossil-fuel carbon sources. Future environmental impact assessments of shorelines and ocean sediments can utilize the  $^{14}\text{C}$  analysis method as demonstrated by Bostic et al. (2018), who traced oil-derived carbon in sand patties following the DWH incident, and by Bosman et al. (2020), who established the baseline isoscapes of surface sediments in the southern Gulf of Mexico.

### **ADVANCEMENTS IN STUDYING HEALTH RISKS FROM INHALED SPILL TOXINS**

The DWH incident created health risks for response workers and others when the spilled oil was subjected to weathering from breaking waves, evaporation, atmospheric forcing, and other processes that contributed to the emission of fumes and the aerosolization of oil and dispersant constituents. Challenges remain in understanding those risks, especially in complex environments such as the turbulent marine-atmospheric boundary layer. In this section, we feature developments related to defining the interactions of waves, oil, and dispersed oil; processes that drive the formation of marine aerosols and their transport; and human exposure risks from aerosolized volatile organic compounds and particulate matter. Related topics are also discussed in Boufadel et al. (2021), Farrington et al. (2021), Quigg et al. (2021), Rullkötter and Farrington (2021), and Sandifer et al.

(2021), all in this issue.

C. Li et al. (2017) built a wave tank to simulate the interactions of waves, oil, and dispersed oil and to investigate subsurface oil droplet evolution (Figure 6). The  $6 \times 0.3 \times 0.6$  m transparent acrylic tank is equipped with a piston-type wave plate that simulates waves from rolling ripples to plunging breakers. A dual-head laser illuminates the flow field and 12 halogen bulbs provide backlighting as three high-speed cameras visualize wave impingement on an oil slick and its breakup and dispersion. Particle image velocimetry characterizes turbulence, and digital inline holography quantifies droplet size distribution. Simulations showed that waves plunge down and splash up multiple times, leaving a series of droplet and bubble clouds behind. Wave structures and subsurface clouds presented similar features for both oil and dispersant-oil treatments, but droplet sizes were very different (1:25 dispersant:oil ratio formed <10  $\mu\text{m}$  droplets compared to oil-only forming 22  $\mu\text{m}$  to mm droplets). Quantifying interfacial tension, viscosity, density, and the effects of wave energy on droplet size distribution bridges small-scale physical processes for slick breakup and large-scale oceanic transport processes. This tank system was used by Afshar-Mohajer et al. (2018, 2019) to generate aerosolized volatile organic compounds and particulate matter that were then measured to provide data for a health risk assessment for oil spill response workers. Cui et al. (2020) used subsurface droplets generated by this tank system for corroboration of test results from a deepwater wave tank system designed to study oil dispersion.

M. Li et al. (2019) developed a hybrid large-eddy model to simulate the transport of aerosolized oil droplets (2.5, 40, 60, and 100  $\mu\text{m}$  diameter) over progressive water waves. The model employs a hybrid spectral and finite-difference method for simulating wind turbulence, a bounded finite-volume method for modeling aerosolized oil transport, and a wave-following coordinate system and



**FIGURE 6.** A custom wave tank was designed for experiments at the Johns Hopkins University Laboratory for Experimental Fluid Dynamics to study the interactions of waves, oil, and dispersed oil, and the evolution of subsurface oil droplets (C. Li et al., 2017). A piston-type wave plate produces a variety of waves, from rolling ripples to plunging breakers. After an oil slick is introduced, its dispersion is visualized and quantified by high-speed cameras, an illuminating laser, and holography. The tank has been used in various oil spill experiments, including one where aerosolized oil spill chemicals emitted by breaking waves were quantified in support of a health risk assessment for spill response workers (Afshar-Mohajer et al., 2019). *Illustration by and used with permission of Cheng Li, Johns Hopkins University. Photo extracted from the Dispatches from the Gulf video and used with permission of Marilyn Weiner, Screenscope Inc.*



computational grid to capture the flow fields adjacent to the waves. Simulations showed that wave-turbulence interaction enhanced the suspension of droplets and expanded the plumes, causing the oil concentration to dilute downstream. Larger droplets tended to resettle on the water, especially during downwelling events. Upwelling events helped to suspend the droplets and, when combined with fast waves, lifted even the 100  $\mu\text{m}$  droplets to 40 m elevation. The 2.5  $\mu\text{m}$  droplets transported like passive tracers, and a large fraction of the 40  $\mu\text{m}$  and 60  $\mu\text{m}$  droplets remained suspended for at least 600 m. The model enables estimations of the order of magnitude of oil droplet concentration near unsteady waves, which are challenging for existing models.

Chandrala et al. (2019) introduced a novel exposure chamber for use in the Real-Time Examination of Cell Exposure (RTECE) system that enables in situ imaging of lung cell cultures during and after exposure to airborne particles. The unique features of the enhanced system include three independently sealed chambers that are adaptable for housing different cell culture optimized, dis-

posable nozzles that provide uniform aerosol deposition and prevent cross-contamination between experiments. The chamber can accommodate different optical components for live imaging of cell morphology and migration, ciliary beat frequency, and more. Validation tests of the enhanced system against existing commercial systems resulted in the same mass deposition and similar initial trends in cellular changes from cigarette smoke. The enhanced system further showed a complex, repeatable time evolution of response, capturing for the first time ciliary beat frequency fluctuations. Data generated with the RTECE system along with field measurements of aerosolized submicron droplets will support a transport model to determine the effects of aerosolized oil and dispersant particles on human lung epithelial cells.

### **DEVELOPMENTS IN INVESTIGATING OIL SPILL IMPACTS ON MARINE LIFE**

As oil from the DWH incident moved from the seafloor through the water column, marine life in affected areas were exposed to hydrocarbons and dis-

persants. Benthic systems were also impacted by oil and dispersants that settled to the seafloor via sinking marine oil snow. Here, we feature novel applications of technology that led to the discovery and monitoring of damaged coral communities and their surrounding habitats. We also describe novel approaches for investigating oil-induced physiological and ecological impacts on commercially and environmentally important fish and marine mammal species that help to provide a more comprehensive understanding of acute and sublethal effects on long-term population dynamics. Topics related to oil spill impacts on marine life are also discussed in Farrington et al. (2021), Halanych et al. (2021), Quigg et al. (2021), Murawski et al. (2021), and Sandifer et al. (2021), all in this issue.

White et al. (2012) combined the use of technologies that can operate in the deep-sea environment with three-dimensional seismic data to find, image, identify, and collect samples of a damaged octocoral community 13 km southwest of the DWH site. Samples of corals, flocculate material, and sediments were collected using customized devices carried by ROV

*Jason II* and *HOV Alvin*. High-resolution chemical analyses were used to fingerprint oil found on or near the affected corals, and those present were associated with Macondo oil (GC×GC-FID identified and quantified biomarkers and GC×GC-MS confirmed biomarker structures). Fisher et al. (2014) discovered more coral communities in the region upon further review of seismic data together with additional data from the AUV *Sentry's* multibeam echosounder surveys and new imagery collected by *Sentry* and a ship-tethered camera system. A Shilling ROV collected high-resolution images and samples of corals, sediments, and associated fauna, which confirmed that there were additional affected communities and expanded the known depth range and areas of spill impacts. Girard and Fisher (2018) developed a timeline of coral recovery or decline using seven years of digitized imagery to document longer-term effects, which may help future coral research.

Ziegwied et al. (2016) launched a new platform for collecting marine mammal acoustic data that integrates Seiche wireless communication and a passive acoustic monitoring (PAM) system with hydrophone arrays, all carried by two autonomous surface vehicles (ASVs). The approach provides a quiet platform (compared to vessel-towed systems), expands the range of frequencies and distances that can be monitored, continuously records acoustic data, and provides real-time monitoring and localizing of marine mammals. The PAM system has a processing electronics module, Wi-Fi connectivity, and 6 TB of storage capacity. The ASV *C-Worker* can operate for 30 days and has a modular payload bay and propulsion and communication systems. The ASV *C-Enduro* can operate for 90 days with its solar panels, wind turbine, and diesel generator. The PAM systems were mounted on the ASVs, launched near the DWH site, and monitored from a support vessel at 500–1,000 m distance. Data collected will be used to understand oil spill impacts on marine mammals

and to advance detection and classification algorithms.

Frasier et al. (2017) used an automated network-based classification technique that employs unsupervised machine learning to develop an algorithm for processing large acoustic data sets of dolphin echolocation clicks. This method addresses the challenge of recognizing patterns in highly variable dolphin clicks by considering a set of clicks as a group of objects that are similar but not identical to one another based on click spectral shape and inter-click interval distributions. By reporting what it finds instead of being told what to look for, the algorithm can identify distinct types of dolphin clicks without prior knowledge of their distinguishing features, allowing for the identification of click types for known and potentially unknown species. Applied to a data set of 52 million dolphin clicks detected in the Gulf of Mexico, the technique identified seven distinct click types, one of which was known and six of which were not. This technique is a step forward in identifying marine mammal species under a big data paradigm that facilitates data analysis for population monitoring after environmental disturbances.

Data generated by the automated network-based classification technique were used by Solsona-Berga et al. (2020) in the development of the DetEdit graphical user interface that accelerates the editing and annotation of automated detections from marine mammal acoustic data sets.

K. Li et al. (2020) developed a three-stage automatic hybrid classifier algorithm that combines a traditional technique with unsupervised clustering to detect species-specific beaked whale calls in acoustic data. First, a spectral energy detector identifies signals in low, medium, and high frequency bands (with the user specifying the frequency for the species of interest), which allows for an initial discrimination of beaked whale calls from sperm whale calls and dolphin clicks. Next, an attribute-discriminator algorithm analyzes signals within the selected frequency band based on prior knowl-

edge of species-specific acoustic properties. Finally, an unsupervised clustering algorithm assigns the remaining signals to species-specific groups based on a hierarchical dendrogram. The method was benchmarked against a manually annotated acoustic data set collected in the northern Gulf of Mexico and achieved a recall (relevancy) rate of 83% for Cuvier's and 78% for Gervais' species. This technique facilitates species-specific analysis, which helped identify differences in habitat preferences of two beaked whale species; it also improves our understanding of how marine mammals respond to environmental disturbances.

Main et al. (2018) extended the development of an aquaculture recirculating system (RAS) and designed an aquatic experimental system to simulate short- or long-term oil exposures of and investigate sublethal impacts on fish (Figure 7). The exposure system consists of nine 500 L fiberglass tanks coated with an isophthalic acid gelcoat that is resistant to chemical and atmospheric agents. The tanks can hold up to 30 fish for 28 days, with each tank system outfitted with a micro bubble diffuser and a flowmeter to maintain oxygen levels and a titanium heat/chill exchange system to control temperature. The tanks are linked to an RAS that includes solid filters, biofilters, oil filters, and UV sterilization filters to maintain water quality and chemistry with acceptable parameters and sumps to remove oil and dispersant. The system operated successfully during experimental trials with Florida pompano, red drum, and southern flounder to evaluate the effects of chronic versus episodic oil-dispersant exposure on fish health. Data from the experiments will be combined with field data to provide a more complete picture of oil spill impacts on fishery populations.

Sherwood et al. (2019) extended work on the aquatic experimental system (Main et al., 2018) and designed a system for sediment exposure trials with flounder to identify nonlethal biomarkers for oil exposure and oxidative stress

and damage. The flow-through system consists of nine 552 L tanks (three control and six exposure tanks, each holding four flounder) linked to an RAS that ensures an uncontaminated seawater renewal of 5,000 L/tank/day to maintain water chemistry and quality. Oiled and control sediment are spread evenly to a depth of ~5 cm on the bottoms of the tanks, then clean seawater is gently added, and sediments are allowed to settle for 72 h. Flounder were sampled after 35-day exposure trials, and a subset were transferred to a clean tank for a 30-day recovery followed by blood and tissue assessments. This system allows for non-lethal biomonitoring of wild fish populations that can inform fishery management decisions following an oil spill. After trials of exposure to oiled sediment and recovery with flounder, Rodgers et al. (2021) observed varied responses in gill and liver tissues from the same individual fish, indicating that tissue type is a key driver of transcriptomic responses to oil.

Nelson et al. (2017) collected real-time measurements of fish cardiac function using blood flow probes inserted in oil-exposed cobia during swim trials in a respirometer chamber. The surgical procedure on anesthetized fish involved exposing the ventral aorta around which a silicone-cuff flow probe was placed with its leads anchored to the lateral body wall and the dorsal surface. After recovery, fish were placed in oil-exposure tanks for 24 h and then transferred to 90 L chamber respirometers for swim trials. The probe leads were connected to a directional pulsed-Doppler blood flow meter to simultaneously measure cardiac function, oxygen consumption, swim performance, and metabolic parameters. After the trial, the fish's blood was infused through the ventral aorta and flow signals were recorded, allowing for calculations of cardiac output, heart rate, and stroke volume. These techniques provided the first measurements of cobia cardiac function as it relates to oil exposure, and results suggest potential negative impacts on fish that could affect their ability to

capture food and escape predation.

Heuer et al. (2019) isolated heart cells from adult mahi-mahi to clarify the mechanisms underlying cardiac function impairment and reduced swim performance following oil exposure, providing the first measurements of cellular contractility in oil-exposed cardiomyocytes from a marine pelagic fish. The hearts of euthanized fish were extracted, and the ventricle was isolated and triturated to free individual cardiomyocytes. An IonOptix Myocyte Contractility system (a perfusion chamber mounted to a microscope attached to a specialized fast-digitizing dimensioning camera) recorded kinetic properties of cardiomyocyte shortening in real time following exposure to various oil concentrations. During oil exposure, cardiomyocytes were stimulated at progressively increasing frequencies representative of heart rates reported in mahi-mahi (~100–180 bpm). In parallel experiments, a patch clamp ampli-

fier (an electrophysiologic technique to study ionic currents in cells) recorded the cardiomyocyte action potential (a brief change in voltage or membrane potential across heart cell membrane). Results provided a link between electrophysiological parameters of oil-induced impairments with a functional consequence. This technique was used by Folkerts et al. (2020) to investigate the impact of flowback water generated by hydraulic fracturing on those same functions in mahi-mahi.

Tarnecki et al. (2016) developed a marine food web matrix of 474 Gulf of Mexico fish species based on diet information obtained from stomach sampling and online information. Diet information was sorted into 89 Atlantis functional groups, then fitted to a statistical model based on the Dirichlet distribution to quantify likely contributions of prey and determine error ranges that reflect diet variability and data quality. Hierarchical cluster analyses performed on the func-



**FIGURE 7.** Laboratory experiments were designed to investigate oil-induced effects on fish to better understand the impacts of oil spill contaminants on marine life. (left) A new aquatic experimental system with nine 500 L fiberglass tanks (blue tanks contain oil and dispersant mixtures) was used to study short- and long-term sublethal impacts of oil spills on Florida pompano, red drum, and southern flounder. To maintain appropriate water quality and chemistry parameters, the tanks are linked to an aquaculture system that provides recirculating filtered water, and sumps are used to remove oil and dispersant (Main et al., 2018). (right) Nonlethal biomarkers for oil exposure and oxidative stress and damage in southern flounder were investigated using a new experimental flow-through system composed of nine 552 L tanks containing oiled or control sediment (Sherwood et al., 2019). Both photos by and used with permission from Kevan L. Main, Mote Marine Laboratory

tional groups helped determine similarity between predator functional groups, and a food web diagram was constructed to visually represent the interconnectivity of predators and prey. A meta-analysis using principal coordinates analyses allowed comparison of this diet matrix to other food webs used in ecosystem modeling. A hindcast model (1980–2010) showed that these data offered an improved fit to observational data and reduced errors in biomass projections in the Ainsworth et al. (2015) food web matrix.

The marine food web matrix was incorporated into the Atlantis model, after which Ainsworth et al. (2018) simulated impacts from the DWH incident on fish guilds and their subsequent recovery, and Court et al. (2020) estimated the direct and total economic impacts associated with changes in commercial and recreational fishing activity following the DWH incident.

Ackleh et al. (2019) developed a non-evolutionary model to describe predator-prey dynamics and then extended it to an evolutionary model under the influence of an environmental toxicant. The discrete-time predator-prey model simulates how prolonged exposure to a toxicant or environmental disturbance, such as an oil spill, may impact predator-prey dynamics when only the prey evolves resistance to the toxicant. The evolutionary model combines population dynamics with an evolving phenotypic trait that measures the amount of toxicant resistance in the prey. Darwinian dynamics are applied so that the evolution of the prey's toxicant resistance occurs on a timescale commensurate with population dynamics (a few generations rather than a few hundred years). Simulations showed that rapid evolution in short-lived species can enable persistence at higher toxicant levels for that species and also for a species with which it interacts. This research was extended in Ackleh et al. (2020) to provide a more in-depth analysis of how the speed of evolution might impact population dynamics in a highly toxic environment.

## EMERGENT DISPERSANT TECHNOLOGIES

Chemical dispersants were applied during the DWH incident to help reduce the harmful vapors emanating from crude oil surface slicks that response workers might be exposed to and to help reduce or prevent coastline oiling. Dispersants help break up an oil slick into small droplets and keep the droplets submerged in the water column to make them more available for biodegradation. However, there are concerns about the risks associated with chemical dispersants to both humans and the environment, prompting research efforts focused on modifications to or substitutes for existing dispersant systems. Emergent dispersant technologies as alternatives to Corexit that show promise as being effective and efficient in oil spill remediation and that are non-toxic to humans and the environment are considered below. Related topics are discussed in Quigg et al. (2021) and Halanych et al. (2021), both in this issue.

Saha et al. (2013) used surface-tunable carbon black (CB) particles as an alternative to Corexit for oil spill remediation. Tests that either added sodium chloride (salt) or reduced pH showed that the particles' hydrophilic-hydrophobic balance can be altered. Salt increased the hydrophilic content the most, indicating that seawater can help make CB particles efficient at spill containment. Comparison tests with Corexit 9500A showed that tuned CB created oil/water emulsions that remained stable in a vial for six months. However, Corexit emulsions destabilized in about an hour and also dispersed water drops into the oil layer, which can hinder oil spill remediation by reducing the energy content in the oil layer, reducing bioremediation efficiency, decreasing the ability to burn the oil, and increasing viscosity and volume that affect removal. Once at the oil/water interface, CB can adsorb polycyclic aromatic hydrocarbons (PAHs) and reduce their transfer to the water column. The availability of CB particles combined with their properties, biocompatibility, and a pat-

ent as a method for cleaning marine oil spills (<https://patents.google.com/patent/US9233862B2/en>) make this a viable alternative technology to Corexit for oil spill application.

Owoseni et al. (2018) formulated a gel-like surfactant with a structure that imparts buoyancy characteristics as a new class of alternative technologies for oil spill remediation. The formulation contains the surfactant components of Corexit (DOSS, Tween 80) and a widely available lecithin component, a phospholipid (L- $\alpha$ -phosphatidylcholine or PC). The combination of Tween 80, DOSS, and PC lowers the oil/water interfacial level. Increased amounts of Tween 80 lead to a transition from sheet-like lamellar structures to spherical, onion-like multilamellar structures. Optical microscopy showed that increasing the Tween 80 content results in smaller droplet sizes, with ~99% being in the 0–25  $\mu\text{m}$  range when Tween 80 is at 27 wt%. The system's buoyancy characteristics provide potential for a floating dispersant that improves adherence to oil in a dynamic ocean environment. Delivery of the gel dispersant as pods, similar to laundry detergent pods, would avoid the use of propylene glycol and the generation of airborne volatile solvents, providing a safer environment for spill responders.

Yu et al. (2019) developed a method for controlling the relative hydrophilic and hydrophobic characteristics of clay halloysite particles by chemically modifying their surfaces using amphiphilic polypeptoids for improved stabilization of oil/water emulsions during spill remediation. Relative to unaltered particles, functionalization with appropriate hydrophobic content effectively lowers the interfacial tension, enhances the particles' thermodynamic propensity to partition at the oil/water interface, and increases the emulsion viscosity, resulting in more stable emulsions. Analysis of emulsions created by functionalized particles showed emulsions lasting 14 days with no change in oil droplet sizes after seven days; those created by pristine par-

ticles had unstable emulsions, and droplet size diameters increased to  $>300\ \mu\text{m}$ . Functionalized particles are not toxic to the hydrocarbon-degrading bacterium *Alcanivorax borkumensis*; instead, they enhance bacterial proliferation compared to less hydrophobic or pristine particles, likely by serving as a nitrogen source, and provide a larger oil/water interfacial area onto which bacteria can better anchor. The use of polypeptoids may improve the viability of clay halloysite particles (<https://patents.google.com/patent/US20180071225A1/en>) for spill response application.

Ojo et al. (2019) designed a stoppering agent using an environmentally benign metal-phenolic network ( $\text{FeCl}_3$ ) to slow the release of surfactant encased within clay halloysite nanotubes for oil spill applications. The stoppering agent addresses the drawback of an almost instantaneous surfactant release when introduced to the oil/water interface, requiring the nanotubes be delivered as a dry material instead of in a liquid solution, which is how dispersants are traditionally applied to an oil slick. The network forms a skin (stopper) around the nanotubes and sequesters the surfactant at a neutral pH value. Changing the pH to an acidic value disassembles the network for a gentle and targeted surfactant release. Tests showed that without the stopper, the surfactant releases in less than an hour, and with the stopper, it releases slowly over 12 h. Droplet size prior to network disassembly was  $182.9 \pm 14\ \mu\text{m}$ , after disassembly it was  $<100\ \mu\text{m}$ , and it then remained unchanged for two weeks. Farinmade et al. (2020) adjusted this system using a thin coating of paraffin wax so that the surfactant release is triggered by contact with oil instead of a pH change. These stoppering techniques may improve the viability of surfactant-loaded halloysite nanotubes (<https://patents.google.com/patent/US20160114303A1/en>) for spill response application.

Other advancements in alternative dispersant technologies include an optimal ratio for a lecithin/Tween 80 (L/T)

surfactant-solvent system (Riehm et al., 2015), which confirmed earlier findings that L/T blends are effective dispersants (Athas et al., 2014; Nyankson et al., 2015), and a thermodynamic model to analyze two-dimensional graphene materials for their emulsification potential at the oil/water interface and the possible creation of graphene-based foams or microsacks to carry lipophilic cargos for spill response (Creighton et al., 2014).

## CONCLUSION

The DWH oil spill was unprecedented in the amounts of oil and gas released and the quantities of dispersants applied near the blowout site at 1,500 m water depth and at the ocean surface. Although mitigation measures were planned for and ready at hand, the severity and unusual circumstances of the accident called for the development of new techniques and approaches, as well as the improvement of existing methods, for mitigation and for investigations of the fate and impacts of the released material and the physical, chemical, and biological processes involved. The 37 technological developments highlighted in this paper are examples of innovations that were introduced during the scientific response to the DWH incident. These innovations resulted from interdisciplinary research and collaborations among national and international entities that represent 49 universities, 10 government agencies, and 17 commercial businesses. The referenced publications for these 37 technological developments have a combined number of more than 2,000 citations (Google Scholar, January 29, 2021).

According to a National Science Board report on invention, knowledge transfer, and innovation, “the relationships among institutions underpin the environment in which ideas become innovations and diffuse through society” (NSF NSB, 2020). The report noted that coauthorship of innovative research in publications that result from collaborative efforts among universities, federal laboratories, and the business sector has increased over the

last decade in both number and citations, which can serve as indicators of knowledge flow and communication that foster innovation. Collaborations that resulted in innovations applied to oil spill research described in this paper as well as in various scientific communications about them help set the stage for future innovations with a wide range of potential applications in the disciplines involved in their development.

Complementary and subsequent research drew on several existing techniques featured here that were applied in the early months following the DWH oil spill and provided fundamental data and information about the newly discovered oil plume and identified and assessed its impacts on sediment and deepwater corals. Those early efforts (Camilli et al., 2010; White et al., 2012; Chanton et al., 2015) reached a high level of awareness within the scientific community as evidenced by their combined number of nearly 1,300 citations (Google Scholar, January 29, 2021).

Several developments discussed here were applied to observations of ocean currents and properties and to observations of the subsurface dynamics of oil and gas droplets, and then contributed to new or improved data about the physical and biogeochemical processes affecting the transport and fate of the spilled oil. These observational data can be incorporated into circulation models to develop more accurate prediction capabilities.

A number of innovations featured in this paper involved laboratory experiments and models that helped to identify and quantify factors that drive the transport and fate of a deepwater oil spill, and their results can improve the simulation of scenarios in support of response decisions. For example, experiments that simulate the formation and evolution of aggregates and flocculant material in the water column provide data and insights that can improve predictions about the sedimentation of oil. Techniques for estimating droplet size distributions with and without dispersants can improve the

simulations of broader oil spill scenarios. Technologies that simulate the generation of aerosolized droplets by breaking waves, the evolution of those droplets over the sea surface, and the effects of inhaled toxins provide data that can support the inclusion of health risk scenarios in response decisions. One of the challenges in oil spill research is to address the scaling of laboratory results to field conditions.

Three techniques featured in this paper improve the processing efficiency of large data sets. The acquisition of large data sets will likely continue with the advancement of efficient ocean acoustic monitoring platforms and the increasing affordability of the high-frequency, high-resolution cameras utilized in several techniques featured in this paper. Research related to the processing of large data sets is likely to be in demand as data scientists and mathematical science occupations are expected to grow 27% by 2029 (US Department of Labor, 2020).

Several innovations were used in oil exposure experiments on fish and used to simulate oil spill scenarios, revealing potential impacts on marine food webs and population dynamics. The developments utilized in these efforts are applicable to a wide range of environmental disturbances that can have cascading negative effects on commercial and recreational fishing and tourism industries that rely on a healthy marine environment. Research that provides information about the type, severity, significance, and duration of oil spill impacts on marine life can inform spill response decisions. Additionally, the development of less-toxic dispersants for spill response could, if utilized, lead to the reduction of oil spill impacts on the marine environment. The challenges for these alternative dispersant technologies include their acceptance, staging, and readying for use in a spill response, particularly on a large scale. As part of their efforts to generate viable dispersant options, academic researchers have cultivated relationships with response agencies and industries

that have testing and production-scale capabilities. These collaborations show promise for improving responses to future oil spills. 

## REFERENCES

- Ackleh, A.S., M.I. Hossain, A. Veprauskas, and A. Zhang. 2019. Persistence and stability analysis of discrete-time predator-prey models: A study of population and evolutionary dynamics. *Journal of Difference Equations and Applications* 25(11):1,568–1,603, <https://doi.org/10.1080/10236198.2019.1669579>.
- Ackleh, A.S., M.I. Hossain, A. Veprauskas, and A. Zhang. 2020. Long-term dynamics of discrete-time predator-prey models: Stability of equilibria, cycles and chaos. *Journal of Difference Equations and Applications* 26(5):693–726, <https://doi.org/10.1080/10236198.2020.1786818>.
- Afshar-Mohajer, N., C. Li, A.M. Rule, J. Katz, and K. Koehler. 2018. A laboratory study of particulate and gaseous emissions from crude oil and crude oil-dispersant contaminated seawater due to breaking waves. *Atmospheric Environment* 179:177–186, <https://doi.org/10.1016/j.atmosenv.2018.02.017>.
- Afshar-Mohajer, N., M.A. Fox, and K. Koehler. 2019. The human health risk estimation of inhaled oil spill emissions with and without adding dispersant. *Science of The Total Environment* 654:924–932, <https://doi.org/10.1016/j.scitotenv.2018.11.110>.
- Ainsworth, C.H., M.J. Schirripa, and H.N. Morzaría-Luna. 2015. *An Atlantis Ecosystem Model for the Gulf of Mexico Supporting Integrated Ecosystem Assessment*. US Department of Commerce, NOAA Technical Memorandum NMFS-SEFSC-676, NOAA Fisheries, Miami, FL, 149 pp.
- Ainsworth, C.H., C.B. Paris, N. Perlin, L.N. Dornberger, W.F. Patterson III, E. Chancellor, S. Murawski, D. Hollander, K. Daly, I.C. Romero, and others. 2018. Impacts of the Deepwater Horizon oil spill evaluated using an end-to-end ecosystem model. *PLoS ONE* 13(1):e0190840, <https://doi.org/10.1371/journal.pone.0190840>.
- Aman, Z.M., C.B. Paris, E.F. May, M.L. Johns, and D. Lindo-Atichati. 2015. High-pressure visual experimental studies of oil-in-water dispersion droplet size. *Chemical Engineering Science* 127:392–400, <https://doi.org/10.1016/j.ces.2015.01.058>.
- Androulidakis, Y., V. Kourafalou, T. Özgökmen, O. Garcia-Pineda, B. Lund, M. Le Hénaff, C. Hu, B.K. Haus, G. Novelli, C. Guigand, and others. 2018. Influence of river-induced fronts on hydrocarbon transport: A multiplatform observational study. *Journal of Geophysical Research Oceans* 123(5):3,259–3,285, <https://doi.org/10.1029/2017JC013514>.
- Androulidakis, Y., V. Kourafalou, L.R. Hole, M. Le Hénaff, and H. Kang. 2020. Pathways of oil spills from potential Cuban offshore exploration: Influence of ocean circulation. *Journal of Marine Science and Engineering* 8(7):535, <https://doi.org/10.3390/jmse8070535>.
- Athas, J.C., K. Jun, C. McCafferty, O. Owoseni, V.T. John, and S.R. Raghavan. 2014. An effective dispersant for oil spills based on food-grade amphiphiles. *Langmuir* 30(31):9,285–9,294, <https://doi.org/10.1021/la502312n>.
- Bacosa, H.P., M. Kamalanathan, J. Cullen, D. Shi, C. Xu, K.A. Schwehr, D. Hala, T.L. Wade, A.H. Knap, P.H. Santschi, and A. Quigg. 2020. Marine snow aggregates are enriched in polycyclic aromatic hydrocarbons (PAHs) in oil contaminated waters: Insights from a mesocosm study. *Journal of Marine Science and Engineering* 8(10):781, <https://doi.org/10.3390/jmse8100781>.
- Barkan, R., M.J. Molemaker, K. Srinivasan, J.C. McWilliams, and E.A. D'Asaro. 2019. The role of horizontal divergence in submesoscale frontogenesis. *Journal of Physical Oceanography* 49(6):1,593–1,618, <https://doi.org/10.1175/JPO-D-18-0162.1>.
- Barker, C.H., V.H. Kourafalou, C.J. Beegle-Krause, M. Boufadel, M.A. Bourassa, S.G. Buschang, Y. Androulidakis, E.P. Chassignet, K.-F. Dagestad, D.G. Danmeier, and others. 2020. Progress in operational modeling in support of oil spill response. *Journal of Marine Science and Engineering* 8(9):668, <https://doi.org/10.3390/jmse8090668>.
- Berenshtein, I., C.B. Paris, N. Perlin, M.M. Alloy, S.B. Joye, and S. Murawski. 2020. Invisible oil beyond the Deepwater Horizon satellite footprint. *Science Advances* 6(7):eaaw8863, <https://doi.org/10.1126/sciadv.aaw8863>.
- Bi, H., Z. Guo, M.C. Benfield, C. Fan, M. Ford, S. Shahrestani, and J.M. Sieracki. 2015. A semi-automated image analysis procedure for in situ plankton imaging systems. *PLoS ONE* 10(5):e0127121, <https://doi.org/10.1371/journal.pone.0127121>.
- Boglaenko, D., and B. Tansel. 2018. Classification of oil-particle interactions in aqueous environments: Aggregate types depending on state of oil and particle characteristics. *Marine Pollution Bulletin* 133:693–700, <https://doi.org/10.1016/j.marpolbul.2018.06.037>.
- Booth, C.P., J.W. Leggoe, and Z.M. Aman. 2019. The use of computational fluid dynamics to predict the turbulent dissipation rate and droplet size in a stirred autoclave. *Chemical Engineering Science* 196:433–443, <https://doi.org/10.1016/j.ces.2018.11.017>.
- Bosman, S.H., P.T. Schwing, R.A. Larson, N.E. Wildermann, G.R. Brooks, I.C. Romero, J.-A. Sanchez-Cabeza, A.C. Ruiz-Fernández, M.L. Machain-Castillo, A. Gracia, and others. 2020. The southern Gulf of Mexico: A baseline radio-carbon isoscape of surface sediments and isotopic excursions at depth. *PLoS ONE* 15(4):e0231678, <https://doi.org/10.1371/journal.pone.0231678>.
- Bostic, J.T., C. Aeppli, R.F. Swarthout, C.M. Reddy, and L.A. Ziolkowski. 2018. Ongoing biodegradation of Deepwater Horizon oil in beach sands: Insights from tracing petroleum carbon into microbial biomass. *Marine Pollution Bulletin* 126:130–136, <https://doi.org/10.1016/j.marpolbul.2017.10.058>.
- Boufadel, M.C., F. Gao, L. Zhao, T. Özgökmen, R. Miller, T. King, B. Robinson, K. Lee, and I. Leifer. 2018. Was the Deepwater Horizon well discharge churn flow? Implications on the estimation of the oil discharge and droplet size distribution. *Geophysical Research Letters* 45(5):2,396–2,403, <https://doi.org/10.1002/2017GL076606>.
- Boufadel, M., A. Bracco, E.P. Chassignet, S.S. Chen, E. D'Asaro, W.K. Dewar, O. Garcia-Pineda, D. Justic, J. Katz, V.H. Kourafalou, and others. 2021. Physical transport processes that affect the distribution of oil in the Gulf of Mexico: Observations and modeling. *Oceanography* 34(1):58–75, <https://doi.org/10.5670/oceanog.2021.117>.
- Brandvik, P.J., Ø. Johansen, E.J. Davies, F. Leirvik, D.F. Krause, P.S. Daling, D. Dunnebie, S. Masutani, I. Nagamine, C. Storey, and others. 2017. Subsea dispersant injection (SSDI): Summary findings from a multi-year research and development industry initiative. Pp. 2,762–2,790 in *International Oil*

- Spill Conference Proceedings*. May 15–18, 2017, Long Beach, CA, American Petroleum Institute, <https://doi.org/10.7901/2169-3358-2017.1.2762>.
- Brandvik, P.J., C. Storey, E.J. Davies, and Ø. Johansen. 2019. Combined releases of oil and gas under pressure: The influence of live oil and natural gas on initial oil droplet formation. *Marine Pollution Bulletin* 140:485–492, <https://doi.org/10.1016/j.marpolbul.2019.01.036>.
- Camilli, R., C.M. Reddy, D.R. Yoerger, B.A.S. Van Mooy, M.V. Jakuba, J.C. Kinsey, C.P. McIntyre, S.P. Sylva, and J.V. Maloney. 2010. Tracking hydrocarbon plume transport and biodegradation at Deepwater Horizon. *Science* 330(6001):201–204, <https://doi.org/10.1126/science.1195223>.
- Carlson, D.F., T. Özgökmen, G. Novelli, C. Guigand, H. Chang, B. Fox-Kemper, J. Mensa, S. Mehta, E. Fredj, H. Huntley, and others. 2018. Surface ocean dispersion observations from the ship-tethered Aerostat Remote Sensing System. *Frontiers in Marine Science* 5:479, <https://doi.org/10.3389/fmars.2018.00479>.
- Chandrala, L.D., N. Afshar-Mohajer, K. Nishida, Y. Ronzhes, V.K. Sidhaye, K. Koehler, and J. Katz. 2019. A device for measuring the in-situ response of human bronchial epithelial cells to airborne environmental agents. *Scientific Reports* 9(7263), <https://doi.org/10.1038/s41598-019-43784-5>.
- Chang, H., H.S. Huntley, A.D. Kirwan Jr., D.F. Carlson, J.A. Mensa, S. Mehta, G. Novelli, T.M. Özgökmen, B. Fox-Kemper, B. Pearson, and others. 2019. Small-scale dispersion in the presence of Langmuir circulation. *Journal of Physical Oceanography* 49(12):3,069–3,085, <https://doi.org/10.1175/JPO-D-19-01071>.
- Chanton, J., T. Zhao, B.E. Rosenheim, S. Joye, S. Bosman, C. Brunner, K.M. Yeager, A.R. Diercks, and D. Hollander. 2015. Using natural abundance radiocarbon to trace the flux of petrocarbon to the seafloor following the Deepwater Horizon oil spill. *Environmental Science & Technology* 49(2):847–854, <https://doi.org/10.1021/es5046524>.
- Chapman, P., S. Socolofsky, and R. Hetland. 2014. From blowout to beach: An integrated modeling approach. Pp. 919–932 in *International Oil Spill Conference Proceedings*, May 5–8, 2014, Savannah, GA, American Petroleum Institute, <https://doi.org/10.7901/2169-3358-2014.1.919>.
- Cheng, K., X. Cheng, Y. Wang, H. Bi, and M.C. Benfield. 2019. Enhanced convolutional neural network for plankton identification and enumeration. *PLoS ONE* 14(7):e0219570, <https://doi.org/10.1371/journal.pone.0219570>.
- Coles, V.J., M.R. Stukel, M.T. Brooks, A. Burd, B.C. Crump, M.A. Moran, J.H. Paul, B.M. Satinsky, P.L. Yager, B.L. Zielinski, and R.R. Hood. 2017. Ocean biogeochemistry modeled with emergent trait-based genomics. *Science* 358(6367):1,149–1,154, <https://doi.org/10.1126/science.aan5712>.
- Court, C., A.W. Hodges, K. Coffey, C.H. Ainsworth, and D. Yoskowitz. 2020. Effects of the Deepwater Horizon oil spill on human communities: Catch and economic impacts. Pp. 569–580 in *Deep Oil Spills*. S. Murawski, C.H. Ainsworth, S. Gilbert, D.J. Hollander, C.B. Paris, M. Schlüter, and D.L. Wetzel, eds, Springer, Cham, Switzerland AG, [https://doi.org/10.1007/978-3-030-11605-7\\_33](https://doi.org/10.1007/978-3-030-11605-7_33).
- Creighton, M.A., Y. Ohata, J. Miyawaki, A. Bose, and R.H. Hurt. 2014. Two-dimensional materials as emulsion stabilizers: Interfacial thermodynamics and molecular barrier properties. *Langmuir* 30(13):3,687–3,696, <https://doi.org/10.1021/la500216n>.
- Cui, F., X. Geng, B. Robinson, T. King, K. Lee, and M.C. Boufadel. 2020. Oil droplet dispersion under a deep-water plunging breaker: Experimental measurement and numerical modeling. *Journal of Marine Science and Engineering* 8(4):230, <https://doi.org/10.3390/jmse8040230>.
- Dagestad, K.-F., J. Röhrs, Ø. Breivik, and B. Ådlandsvik. 2018. OpenDrift v1.0: A generic framework for trajectory modelling. *Geoscientific Model Development* 11:1,405–1,420, <https://doi.org/10.5194/gmd-11-1405-2018>.
- D'Asaro, E.A., A.Y. Shcherbina, J.M. Klymak, J. Molemaker, G. Novelli, C.M. Guigand, A.C. Haza, B.K. Haus, E.H. Ryan, G.A. Jacobs, and others. 2018. Ocean convergence and the dispersion of flotsam. *Proceedings of the National Academy of Sciences of the United States of America* 115(6):1,162–1,167, <https://doi.org/10.1073/pnas.1718453115>.
- Daly, K.L., A.C. Vaz, and C.B. Paris. 2020. Physical processes influencing the sedimentation and lateral transport of MOSSFA in the NE Gulf of Mexico. Pp. 300–314 in *Scenarios and Responses to Future Deep Oil Spills*. S. Murawski, C.H. Ainsworth, S. Gilbert, D.J. Hollander, C.B. Paris, M. Schlüter, and D.L. Wetzel, eds, Springer, Cham, Switzerland AG, [https://doi.org/10.1007/978-3-030-12963-7\\_18](https://doi.org/10.1007/978-3-030-12963-7_18).
- Davies, E.J., P.J. Brandvik, F. Leirvik, and R. Nepstad. 2017. The use of wide-band transmittance imaging to size and classify suspended particulate matter in seawater. *Marine Pollution Bulletin* 115:105–114, <https://doi.org/10.1016/j.marpolbul.2016.11.063>.
- Diercks, A.R., R.C. Highsmith, V.L. Asper, D. Joung, Z. Zhou, L. Guo, A.M. Shiller, S.B. Joye, A.P. Teske, N. Guinasso, and others. 2010. Characterization of subsurface polycyclic aromatic hydrocarbons at the Deepwater Horizon site. *Geophysical Research Letters* 37(20), <https://doi.org/10.1029/2010GL045046>.
- Dissanayake, A.L., J. Gros, and S.A. Socolofsky. 2018a. Integral models for bubble, droplet, and multiphase plume dynamics in stratification and crossflow. *Environmental Fluid Mechanics* 18:1,167–1,202, <https://doi.org/10.1007/s10652-018-9591-y>.
- Dissanayake, A.L., A.B. Burd, K.L. Daly, S. Francis, and U. Passow. 2018b. Numerical modeling of the interactions of oil, marine snow, and riverine sediments in the ocean. *Journal of Geophysical Research Oceans* 123(8):5,388–5,405, <https://doi.org/10.1029/2018JC013790>.
- Doyle, S.M., E.A. Whitaker, V. De Pascuale, T.L. Wade, A.H. Knap, P.H. Santschi, A. Quigg, and J.B. Sylvan. 2018. Rapid formation of microbe-oil aggregates and changes in community composition in coastal surface water following exposure to oil and the dispersant Corexit. *Frontiers in Microbiology* 9:689, <https://doi.org/10.3389/fmicb.2018.00689>.
- Dukhovskoy, D.S., S.L. Morey, E.P. Chassignet, X. Chen, V.J. Coles, L. Cui, K.C. Harris, R. Hetland, T.-J. Hsu, A.J. Manning, and others. 2021. Development of the CSOMIO Coupled Ocean-Sediment-Biology-Model. *Frontiers in Marine Science*, <https://doi.org/10.3389/fmars.2021.629299>.
- Farinmade, A., O.F. Ojo, J. Trout, J. He, V. John, D.A. Blake, Y.M. Lvov, D. Zhang, D. Nguyen, and A. Bose. 2020. Targeted and stimulus-responsive delivery of surfactant to the oil-water interface for applications in oil spill remediation. *ACS Applied Materials & Interfaces* 12(1):1,840–1,849, <https://doi.org/10.1021/acsami.9b17254>.
- Farrington, J.W., E.B. Overton, and U. Passow. 2021. Biogeochemical processes affecting the fate of discharged Deepwater Horizon gas and oil: New insights and remaining gaps in our understanding. *Oceanography* 34(1):76–97, <https://doi.org/10.5670/oceanog.2021.118>.
- Fisher, C.R., P.-Y. Hsing, C.L. Kaiser, D.R. Yoerger, H.H. Roberts, W.W. Shedd, E.E. Cordes, T.M. Shank, S.P. Berlet, M.G. Saunders, and others. 2014. Footprint of Deepwater Horizon blowout impact to deep-water coral communities. *Proceedings of the National Academy of Sciences of the United States of America* 111(32):11,744–11,749, <https://doi.org/10.1073/pnas.1403492111>.
- Folkerts, E.J., R.M. Heuer, S. Flynn, J.D. Stieglitz, D.D. Benetti, D.S. Alessi, G.G. Goss, and M. Grosell. 2020. Exposure to hydraulic fracturing flowback water impairs mahi-mahi (*Coryphaena hippurus*) cardiomyocyte contractile function and swimming performance. *Environmental Science & Technology* 54(21):13,579–13,589, <https://doi.org/10.1021/acs.est.0c02719>.
- Frasier, K.E., M.A. Roch, M.S. Soldevilla, S.M. Wiggins, L.P. Garrison, and J.A. Hildebrand. 2017. Automated classification of dolphin echolocation click types from the Gulf of Mexico. *PLoS Computational Biology* 13(12):e1005823, <https://doi.org/10.1371/journal.pcbi.1005823>.
- Garcia-Pineda, O., Y. Androulidakis, M. Le Hénaff, V. Kourafalou, L.R. Hole, H. Kang, G. Staples, E. Ramirez, and L. DiPinto. 2020. Measuring oil residence time with GPS-drifters, satellites, and Unmanned Aerial Systems (UAS). *Marine Pollution Bulletin* 150:110644, <https://doi.org/10.1016/j.marpolbul.2019.110644>.
- Girard, F., and C.R. Fisher. 2018. Long-term impact of the Deepwater Horizon oil spill on deep-sea corals detected after seven years of monitoring. *Biological Conservation* 225:117–127, <https://doi.org/10.1016/j.biocon.2018.06.028>.
- Gonçalves, R.C., M. Iskandarani, T. Özgökmen, and W.C. Thacker. 2019. Reconstruction of sub-mesoscale velocity field from surface drifters. *Journal of Physical Oceanography* 49(4):941–958, <https://doi.org/10.1175/JPO-D-18-0025.1>.
- Gordon, C., K. Fennel, C. Richards, L.K. Shay, and J.K. Brewster. 2020. Can ocean community production and respiration be determined by measuring high-frequency oxygen profiles from autonomous floats? *Biogeosciences* 17(15):4,119–4,134, <https://doi.org/10.5194/bg-17-4119-2020>.
- Gros, J., S.A. Socolofsky, A.L. Dissanayake, I. Jun, L. Zhao, M.C. Boufadel, C.M. Reddy, and J.S. Arey. 2017. Petroleum dynamics in the sea and influence of subsea dispersant injection during Deepwater Horizon. *Proceedings of the National Academy of Sciences of the United States of America* 114(38):10,065–10,070, <https://doi.org/10.1073/pnas.1612518114>.
- Gros, J., J.S. Arey, S.A. Socolofsky, and A.L. Dissanayake. 2020. Dynamics of live oil droplets and natural gas bubbles in deep water. *Environmental Science & Technology* 54(19):11,865–11,875, <https://doi.org/10.1021/acs.est.9b06242>.
- Halanych, K.M., C.H. Ainsworth, E.E. Cordes, R.E. Dodge, M. Huettel, I.A. Mendelssohn, S.A. Murawski, C.B. Paris-Limouzy, P.T. Schwing, R.F. Shaw, and T. Sutton. 2021. Effects of petroleum by-products and dispersants on ecosystems. *Oceanography* 34(1):152–163, <https://doi.org/10.5670/oceanog.2021.123>.
- Heuer, R.M., G.L.J. Galli, H.A. Shiels, L.A. Fieber, G.K. Cox, E.M. Mager, J.D. Stieglitz, D.D. Benetti, M. Grosell, and D.A. Crossley II. 2019. Impacts of Deepwater Horizon crude oil on mahi-mahi (*Coryphaena hippurus*)

- heart cell function. *Environmental Science & Technology* 53(16):9,895–9,904, <https://doi.org/10.1021/acs.est.9b03798>.
- Hole, L.R., K.-F. Dagestad, J. Röhrs, C. Wetters, V.H. Kourafalou, Y. Andrulidakis, H. Kang, M. Le Hénaff, and O. Garcia-Pineda. 2019. The Deepwater Horizon oil slick: Simulations of river front effects and oil droplet size distribution. *Journal of Marine Science and Engineering* 7(10):329, <https://doi.org/10.3390/jmse7100329>.
- Jones, L., and M.H. Garcia. 2018. Development of a rapid response riverine oil-particle aggregate formation, transport, and fate model. *Journal of Environmental Engineering* 144(12):04018125, [https://doi.org/10.1061/\(ASCE\)EE.1943-7870.0001470](https://doi.org/10.1061/(ASCE)EE.1943-7870.0001470).
- Knap, A.H., T.D. Sleeter, R.E. Dodge, S.C. Wyers, H.R. Frith, and S.R. Smith. 1983. The effects of oil spills and dispersant use on corals: A review and multi-disciplinary experimental approach. *Oil and Petroleum Pollution* 1(3):157–169, [https://doi.org/10.1016/S0143-7127\(83\)90134-5](https://doi.org/10.1016/S0143-7127(83)90134-5).
- Kujawinski, E.B., M.C. Kido Soule, D.L. Valentine, A.K. Boysen, K. Longnecker, and M.C. Redmond. 2011. Fate of dispersants associated with the Deepwater Horizon oil spill. *Environmental Science & Technology* 45(4):1,298–1,306, <https://doi.org/10.1021/es103838p>.
- Laxague, N.J.M., T.M. Özgökmen, B.K. Haus, G. Novelli, A. Shcherbina, P. Sutherland, C.M. Guigand, B. Lund, S. Mehta, M. Alday, and J. Molemaker. 2018. Observations of near-surface current shear help describe oceanic oil and plastic transport. *Geophysical Research Letters* 45(1):245–249, <https://doi.org/10.1002/2017GL075891>.
- Leonte, M., B. Wang, S.A. Socolofsky, S. Mau, J.A. Breier, and J.D. Kessler. 2018. Using carbon isotope fractionation to constrain the extent of methane dissolution into the water column surrounding a natural hydrocarbon gas seep in the northern Gulf of Mexico. *Geochemistry, Geophysics, Geosystems* 19(11):4,459–4,475, <https://doi.org/10.1029/2018GC007705>.
- Li, C., J. Miller, J. Wang, S.S. Koley, and J. Katz. 2017. Size distribution and dispersion of droplets generated by impingement of breaking waves on oil slicks. *Journal of Geophysical Research Oceans* 122(10):7,938–7,957, <https://doi.org/10.1002/2017JC013193>.
- Li, K., N.A. Sidorovskaia, and C.O. Tiemann. 2020. Model-based unsupervised clustering for distinguishing Cuvier's and Gervais's beaked whales in acoustic data. *Ecological Informatics* 58:101094, <https://doi.org/10.1016/j.ecoinf.2020.101094>.
- Li, M., Z. Zhao, Y. Pandya, G.V. Iungo, and D. Yang. 2019. Large-eddy simulations of oil droplet aerosol transport in the marine atmospheric boundary layer. *Atmosphere* 10(8):459, <https://doi.org/10.3390/atmos10080459>.
- Lindo-Atichati, D., C.B. Paris, M. Le Hénaff, M. Schedler, A.G. Valladares-Juárez, and R. Müller. 2016. Simulating the effects of droplet size, high-pressure biodegradation, and variable flow rate on the subsea evolution of deep plumes from the Macondo blowout. *Deep Sea Research Part II* 129:301–310, <https://doi.org/10.1016/j.dsr2.2014.01.011>.
- Lund, B., B.K. Haus, J. Horstmann, H.C. Graber, R. Carrasco, N.J.M. Laxague, G. Novelli, C.M. Guigand, and T.M. Özgökmen. 2018. Near-surface current mapping by shipboard marine X-band radar: A validation. *Journal of Atmospheric and Oceanic Technology* 35(5):1,077–1,090, <https://doi.org/10.1175/JTECH-D-17-0154.1>.
- Main, K.L., D.L. Wetzel, R. Grams, M.J. Nystrom, K. Niebuhr, and J. Lewis. 2018. Utilizing recirculating aquaculture systems to evaluate the impact of oil toxicity on marine fishes: Design and operation of a large-scale experimental system. *Marine Technology Society Journal* 52(6):23–31, <https://doi.org/10.4031/MTSJ.52.6.2>.
- Murawski, S.A., M. Grosell, C. Smith, T. Sutton, K.M. Halanych, R.F. Shaw, and C.A. Wilson. 2021. Impacts of petroleum, petroleum components, and dispersants on organisms and populations. *Oceanography* 34(1):136–151, <https://doi.org/10.5670/oceanog.2021.122>.
- Nelson, D., J.D. Stieglitz, G.K. Cox, R.M. Heuer, D.D. Benetti, M. Grosell, and D.A. Crossley II. 2017. Cardio-respiratory function during exercise in the coho, *Rachycentron canadum*: The impact of crude oil exposure. *Comparative Biochemistry and Physiology Part C: Toxicology & Pharmacology* 201:58–65, <https://doi.org/10.1016/j.cbpc.2017.08.006>.
- North, E.W., E.E. Adams, A.E. Thessen, Z. Schlag, R. He, S.A. Socolofsky, S.M. Masutani, and S.D. Peckham. 2015. The influence of droplet size and biodegradation on the transport of subsurface oil droplets during the Deepwater Horizon spill: A model sensitivity study. *Environmental Research Letters* 10(2):024016, <https://doi.org/10.1088/1748-9326/10/2/024016>.
- Novelli, G., C.M. Guigand, C. Cousin, E.H. Ryan, N.J.M. Laxague, H. Dai, B.K. Haus, and T.M. Özgökmen. 2017. A biodegradable surface drifter for ocean sampling on a massive scale. *Journal of Atmospheric and Oceanic Technology* 34(11):2,509–2,532, <https://doi.org/10.1175/JTECH-D-17-0055.1>.
- Novelli, G., C.M. Guigand, M.C. Bouffadel, and T.M. Özgökmen. 2020. On the transport and land-fall of marine oil spills, laboratory and field observations. *Marine Pollution Bulletin* 150:110805, <https://doi.org/10.1016/j.marpolbul.2019.110805>.
- NSF NSB (National Science Foundation, National Science Board). 2020. Invention, Knowledge Transfer, and Innovation. *Science and Engineering Indicators 2020*. NSB-2020-4, Alexandria, VA, <https://nces.nsf.gov/pubs/nsb20204/>.
- Nyankson, E., O. Owoseni, V.T. John, and R.B. Gupta. 2015. Surfactant-loaded halloysite clay nanotube dispersants for crude oil spill remediation. *Industrial & Engineering Chemistry Research* 54(38):9,328–9,341, <https://doi.org/10.1021/acs.iecr.5b02032>.
- Ojo, O.F., A. Farinmade, J. Trout, M. Omarova, J. He, V. John, D.A. Blake, Y.M. Lvov, D. Zhang, D. Nguyen, and A. Bose. 2019. Stoppers and skins on clay nanotubes help stabilize oil-in-water emulsions and modulate the release of encapsulated surfactants. *ACS Applied Nano Materials* 2(6):3,490–3,500, <https://doi.org/10.1021/acsanm.9b00469>.
- Owoseni, O., Y. Zhang, M. Omarova, X. Li, J. Lal, G.L. McPherson, S.R. Raghavan, A. Bose, and V.T. John. 2018. Microstructural characteristics of surfactant assembly into a gel-like mesophase for application as an oil spill dispersant. *Journal of Colloid and Interface Science* 524:279–288, <https://doi.org/10.1016/j.jcis.2018.03.089>.
- Passow, U., J. Sweet, S. Francis, C. Xu, A.L. Dissanayake, Y.-Y. Lin, P.H. Santschi, and A. Quigg. 2019. Incorporation of oil into diatom aggregates. *Marine Ecology Progress Series* 612:65–86, <https://doi.org/10.3354/meps12881>.
- Perlin, N., C.B. Paris, I. Berenshtein, A.C. Vaz, R. Faillietaz, Z.M. Aman, P.T. Schwing, I.C. Romero, M. Schlüter, A. Liese, and others. 2020. Far-field modeling of a deep-sea blowout: Sensitivity studies of initial conditions, biodegradation, sedimentation, and subsurface dispersant injection on surface slicks and oil plume concentrations. Pp. 170–192 in *Deep Oil Spills*. S. Murawski, C.H. Ainsworth, S. Gilbert, D.J. Hollander, C.B. Paris, M. Schlüter, and D.L. Wetzel, eds, Springer, Cham, Switzerland AG, [https://doi.org/10.1007/978-3-030-11605-7\\_11](https://doi.org/10.1007/978-3-030-11605-7_11).
- Quigg, A., J.W. Farrington, S. Gilbert, S.A. Murawski, and V.T. John. 2021. A decade of GoMRI dispersant science: Lessons learned and recommendations for the future. *Oceanography* 34(1):98–111, <https://doi.org/10.5670/oceanog.2021.119>.
- Razaz, M., D. Di Iorio, B. Wang, S. Daneshgar Asl, and A.M. Thurnherr. 2020. Variability of a natural hydrocarbon seep and its connection to the ocean surface. *Scientific Reports* 10:12654, <https://doi.org/10.1038/s41598-020-68807-4>.
- Reddy, C.M., J.S. Arey, J.S. Seewald, S.P. Sylva, K.L. Lemkau, R.K. Nelson, C.A. Carmichael, C.P. McIntyre, J. Fenwick, G.T. Ventura, and others. 2012. Composition and fate of gas and oil released to the water column during the Deepwater Horizon oil spill. *Proceedings of the National Academy of Sciences of the United States of America* 109(50):20,229–20,234, <https://doi.org/10.1073/pnas.1101242108>.
- Riehm, D.A., J.E. Neilsen, G.D. Bothun, V.T. John, S.R. Raghavan, and A.V. McCormick. 2015. Efficient dispersion of crude oil by blends of food-grade surfactants: Toward greener oil-spill treatments. *Marine Pollution Bulletin* 101(1):92–97, <https://doi.org/10.1016/j.marpolbul.2015.11.012>.
- Rodgers, M.L., T.A. Sherwood, A.M. Tarnecki, R.J. Griffith, and D.L. Wetzel. 2021. Characterizing transcriptomic responses of southern flounder (*Paralichthys lethostigma*) chronically exposed to Deepwater Horizon oiled sediments. *Aquatic Toxicology* 230:105716, <https://doi.org/10.1016/j.aquatox.2020.105716>.
- Rullkötter, J., and J.W. Farrington. 2021. What was released? Assessing the physical properties and chemical composition of petroleum and products of burned oil. *Oceanography* 34(1):44–57, <https://doi.org/10.5670/oceanog.2021.116>.
- Saha, A., A. Nikova, P. Venkataraman, V.T. John, and A. Bose. 2013. Oil emulsification using surface-tunable carbon black particles. *ACS Applied Materials & Interfaces* 5(8):3,094–3,100, <https://doi.org/10.1021/am3032844>.
- Sandifer, P.A., A. Ferguson, M.L. Finucane, M. Partyka, H.M. Solo-Gabriele, A.H. Walker, K. Wowk, R. Caffey, and D. Yoskowitz. 2021. Human health and socio-economic effects of the Deepwater Horizon oil spill in the Gulf of Mexico. *Oceanography* 34(1):174–191, <https://doi.org/10.5670/oceanog.2021.125>.
- Shahrestani, S., H. Bi, V. Lyubchich, and K.M. Boswell. 2017. Detecting a nearshore fish parade using the adaptive resolution imaging sonar (ARIS): An automated procedure for data analysis. *Fisheries Research* 191:190–199, <https://doi.org/10.1016/j.fishres.2017.03.013>.
- Shay, L.K., J.K. Brewster, B. Jaimes, C. Gordon, K. Fennel, P. Furze, H. Fargher, and R. He. 2019. Physical and biochemical structure measured by APEX-EM floats. Pp.1–6 in *2019 IEEE/OES Twelfth Current, Waves and Turbulence Measurement (CWTM)*. March 10–13, 2019, Institute of Electrical and Electronic Engineers, San Diego, CA, <https://doi.org/10.1109/CWTM43797.2019.8955168>.
- Sherwood, T.A., R.L. Medvecky, C.A. Miller, A.M. Tarnecki, R.W. Schloesser, K.L. Main, C.L. Mitchelmore, and D.L. Wetzel. 2019. Nonlethal biomarkers of oxidative stress in oiled sediment exposed southern flounder (*Paralichthys lethostigma*): Utility for field-base monitoring exposure

- and potential recovery. *Environmental Science & Technology* 53(24):14,734–14,743, <https://doi.org/10.1021/acs.est.9b05930>.
- Shi, D., G. Bera, A.H. Knap, A. Quigg, I. Al Atwah, G. Gold-Bouchot, and T.L. Wade. 2020. A mesocosm experiment to determine half-lives of individual hydrocarbons in simulated oil spill scenarios with and without the dispersant, Corexit. *Marine Pollution Bulletin* 151:110804, <https://doi.org/10.1016/j.marpolbul.2019.110804>.
- Socolofsky, S.A., E.E. Adams, and C.R. Sherwood. 2020. Formation dynamics of subsurface hydrocarbon intrusions following the Deepwater Horizon blowout. *Geophysical Research Letters* 38(9), <https://doi.org/10.1029/2011GL047174>.
- Socolofsky, S.A., J. Gros, E. North, M.C. Boufadel, T.F. Parkerton, and E.E. Adams. 2019. The treatment of biodegradation in models of sub-surface oil spills: A review and sensitivity study. *Marine Pollution Bulletin* 143:204–219, <https://doi.org/10.1016/j.marpolbul.2019.04.018>.
- Solsona-Berga, A., K.E. Frasier, S. Baumann-Pickering, S.M. Wiggins, and J.A. Hildebrand. 2020. DetEdit: A graphical user interface for annotating and editing events detected in long-term acoustic monitoring data. *PLoS Computational Biology* 16(1):e1007598, <https://doi.org/10.1371/journal.pcbi.1007598>.
- Tarnecki, J.H., A.A. Wallace, J.D. Simons, and C.H. Ainsworth. 2016. Progression of a Gulf of Mexico food web supporting Atlantis ecosystem model development. *Fisheries Research* 179:237–250, <https://doi.org/10.1016/j.fishres.2016.02.023>.
- US Department of Labor, Bureau of Labor Statistics, Employment Projections Program. 2020. *Fastest growing occupations*, <https://www.bls.gov/emp/tables/fastest-growing-occupations.htm>.
- Valentine, D.L., G.B. Fisher, S.C. Bagby, R.K. Nelson, C.M. Reddy, S.P. Sylva, and M.A. Woo. 2014. Fallout plume of submerged oil from Deepwater Horizon. *Proceedings of the National Academy of Sciences of the United States of America* 111(45):15,906–15,911, <https://doi.org/10.1073/pnas.1414873111>.
- Wade, T.L., M. Morales-McDevitt, G. Bera, D. Shi, S. Sweet, B. Wang, G. Gold-Bouchot, A. Quigg, and A.H. Knap. 2017. A method for the production of large volumes of WAF and CEWAF for dosing mesocosms to understand marine oil snow formation. *Heliyon* 3(10):e00419, <https://doi.org/10.1016/j.heliyon.2017.e00419>.
- Wang, B., and S.A. Socolofsky. 2015. A deep-sea, high-speed, stereoscopic imaging system for in situ measurement of natural seep bubble and droplet characteristics. *Deep Sea Research Part I* 104:134–148, <https://doi.org/10.1016/j.dsr.2015.08.001>.
- Wang, B., I. Jun, S.A. Socolofsky, S.F. DiMarco, and J.D. Kessler. 2020. Dynamics of gas bubbles from a submarine hydrocarbon seep within the hydrate stability zone. *Geophysical Research Letters* 47(18):e2020GL089256, <https://doi.org/10.1029/2020GL089256>.
- Warner, J.C., B. Armstrong, R. He, and J.B. Zambon. 2010. Development of a Coupled Ocean-Atmosphere-Wave-Sediment Transport (COAWST) Modeling System. *Ocean Modelling* 35(3):230–244, <https://doi.org/10.1016/j.ocemod.2010.07.010>.
- White, H.K., P.-Y. Hsing, W. Cho, T.M. Shank, E.E. Cordes, A.M. Quattrini, R.K. Nelson, R. Camilli, A.W.J. Demopoulos, C.R. German, and others. 2012. Impact of the Deepwater Horizon oil spill on a deep-water coral community in the Gulf of Mexico. *Proceedings of the National Academy of Sciences of the United States of America* 109(50):20,303–20,308, <https://doi.org/10.1073/pnas.1118029109>.
- Ye, L., A.J. Manning, T.-J. Hsu, S. Morey, E.P. Chassignet, and T.A. Ippolito. 2018. Novel application of laboratory instrumentation characterizes mass settling dynamics of oil-mineral aggregates (OMAs) and oil-mineral-microbial interactions. *Marine Technology Society Journal* 52(6):87–90, <https://doi.org/10.4031/MTSJ.52.6.14>.
- Ye, L., A.J. Manning, and T.-J. Hsu. 2020. Oil-mineral flocculation and settling velocity in saline water. *Water Research* 173:115569, <https://doi.org/10.1016/j.watres.2020.115569>.
- Yu, T., L.T. Swintoniewski, M. Omarova, M.-C. Li, I.I. Negulescu, N. Jiang, O.A. Darvish, A. Panchal, D.A. Blake, Q. Wu, and others. 2019. Investigation of amphiphilic polypeptoid-functionalized halloysite nanotubes as emulsion stabilizer for oil spill remediation. *ACS Applied Materials & Interfaces* 11(31):27,944–27,953, <https://doi.org/10.1021/acsami.9b08623>.
- Zhao, L., J. Torlapati, M.C. Boufadel, T. King, B. Robinson, and K. Lee. 2014a. VDROD: A comprehensive model for droplet formation of oil and gases in liquids—Incorporation of the interfacial tension and droplet viscosity. *Chemical Engineering Journal* 253:93–106, <https://doi.org/10.1016/j.cej.2014.04.082>.
- Zhao, L., M.C. Boufadel, S.A. Socolofsky, E. Adams, T. King, and K. Lee. 2014b. Evolution of droplets in subsea oil and gas blowouts: Development and validation of the numerical model VDROD-J. *Marine Pollution Bulletin* 83(1):58–69, <https://doi.org/10.1016/j.marpolbul.2014.04.020>.
- Zhao, L., M.C. Boufadel, E. Adams, S.A. Socolofsky, T. King, K. Lee, and T. Nedwed. 2015. Simulation of scenarios of oil droplet formation from the Deepwater Horizon blowout. *Marine Pollution Bulletin* 101(1):304–319, <https://doi.org/10.1016/j.marpolbul.2015.10.068>.
- Zhao, L., M.C. Boufadel, X. Geng, K. Lee, T. King, B. Robinson, and F. Fitzpatrick. 2016. A-DROP: A predictive model for the formation of oil particle aggregates (OPAs). *Marine Pollution Bulletin* 106(1–2):245–259, <https://doi.org/10.1016/j.marpolbul.2016.02.057>.
- Zhao, L., M.C. Boufadel, T. King, B. Robinson, F. Gao, S.A. Socolofsky, and K. Lee. 2017. Droplet and bubble formation of combined oil and gas releases in subsea blowouts. *Marine Pollution Bulletin* 120(1–2):203–216, <https://doi.org/10.1016/j.marpolbul.2017.05.010>.
- Ziegwied, A.T., V. Dobbin, S. Dyer, C. Pierpoint, and N. Sidorovskaia. 2016. Using autonomous surface vehicles for passive acoustic monitoring (PAM). Pp. 1–5 in *OCEANS 2016 MTS/IEEE Monterey*, September 19–23, 2016, Monterey, CA, Institute of Electrical and Electronic Engineers, <https://doi.org/10.1109/OCEANS.2016.7761380>.

USA. Jürgen Rullkötter is Professor Emeritus, Carl von Ossietzky University Oldenburg, Oldenburg, Germany. Dana Yoerger is Senior Scientist, Woods Hole Oceanographic Institution, Woods Hole, MA, USA.

## ARTICLE CITATION

Dannreuther, N.M., D. Halpern, J. Rullkötter, and D. Yoerger. 2021. Technological developments since the Deepwater Horizon oil spill. *Oceanography* 34(1):192–211, <https://doi.org/10.5670/oceanog.2021.126>.

## COPYRIGHT & USAGE

This is an open access article made available under the terms of the Creative Commons Attribution 4.0 International License (<https://creativecommons.org/licenses/by/4.0/>), which permits use, sharing, adaptation, distribution, and reproduction in any medium or format as long as users cite the materials appropriately, provide a link to the Creative Commons license, and indicate the changes that were made to the original content.

## ACKNOWLEDGMENTS

This research was made possible by the Gulf of Mexico Research Initiative. We gratefully acknowledge and thank the authors of publications referenced in this paper for providing reviews of individual techniques described here. We are thankful to the anonymous reviewers of this paper who provided excellent recommendations that improved its quality.

## AUTHORS

Niide Maggie Dannreuther (maggied@ngi.msstate.edu) is Coordinator, Northern Gulf Institute, Mississippi State University, Stennis Space Center, MS, USA. David Halpern is Visiting Researcher, Scripps Institution of Oceanography, University of California San Diego, La Jolla, CA,